DMFT simulations of ultracold fermions in optical lattices

Nils Blümer and Elena Gorelik

Outline

Methods:
- DMFT, Hirsch-Fye quantum Monte Carlo (HF-QMC)
- Quasi-CT algorithm: multigrid HF-QMC

Ultracold fermions:
- Model systems for strongly correlated materials
- Paramagnetic Mott transitions in 3-flavor mixtures
  - Impact of the lattice type
- Melting of an antiferromagnet in an optical trap

Summary and outlook

Support by DFG within SFB/TR 49

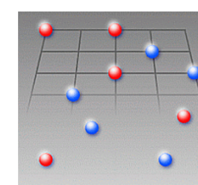

Methods: DMFT and HF-QMC

Target: Hubbard-type models $H = -\sum_{(i,j),\sigma} t_{ij} (c^\dagger_{i\sigma} c_{j\sigma} + \text{h.c.}) + U \sum_i n_{i\uparrow} n_{i\downarrow}$

Dynamical mean-field theory (DMFT): local self-energy $\Sigma(\boldsymbol{k},\omega) \equiv \Sigma(\omega)$

[Metzner, Vollhardt, PRL (1989), Georges, Kotliar, PRL (1992), Jarrell, PRL (1992)]

+ non-perturbative $\rightsquigarrow$ valid at MIT
+ dynamical on-site correlations preserved
+ in thermodynamic limit

+/− exact for coordination $Z \to \infty$

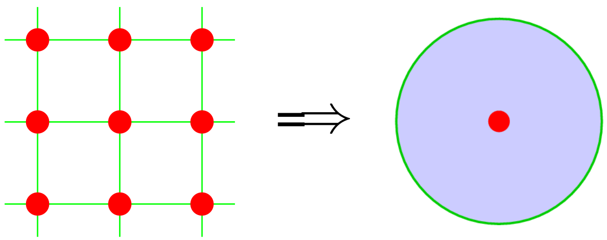

Methods: DMFT and HF-QMC

Target: Hubbard-type models $H = -\sum_{(i,j),\sigma} t_{ij}\,(c^{\dagger}_{i\sigma} c_{j\sigma} + \text{h.c.}) + U \sum_{i} n_{i\uparrow} n_{i\downarrow}$

Dynamical mean-field theory (DMFT): local self-energy $\Sigma(\boldsymbol{k},\omega) \equiv \Sigma(\omega)$

[Metzner, Vollhardt, PRL (1989), Georges, Kotliar, PRL (1992), Jarrell, PRL (1992)]

+ non-perturbative $\rightsquigarrow$ valid at MIT
+ dynamical on-site correlations preserved
+ in thermodynamic limit

+/− exact for coordination $Z \to \infty$

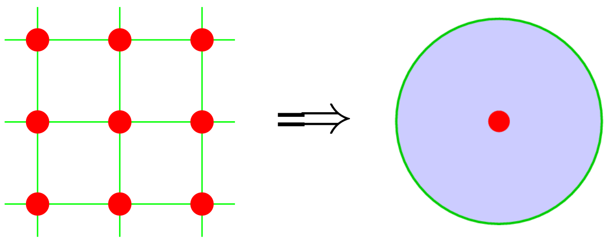

Numerically exact impurity solvers:

- Quantum Monte Carlo (QMC)
- Exact diagonalization (ED; large finite-size errors)
- Numerical renormalization group (NRG; 1-2 bands)
- Density matrix renormalization group (DMRG)

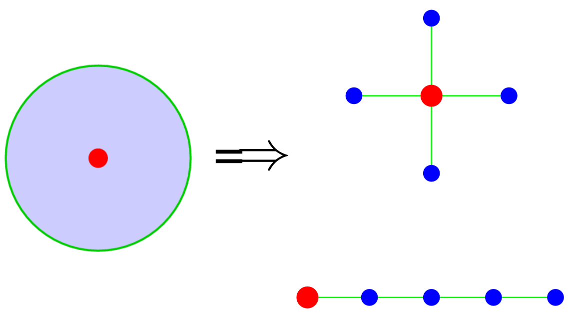

Auxiliary-field QMC algorithm [Hirsch, Fye (1986)]

Green function G in imaginary time (fermionic Grassmann variables ψ, ψ^*):

$$G_\sigma(\tau_2 - \tau_1) = \frac{1}{\mathcal{Z}} \int \mathcal{D}[\psi]\,\mathcal{D}[\psi^*]\;\; \psi_\sigma(\tau_1)\psi^*_\sigma(\tau_2)\;\exp\Big[\mathcal{A}_0 - U \sum_{\sigma\sigma'} \int_0^\beta d\tau\, \psi^*_\sigma \psi_\sigma \psi^*_{\sigma'} \psi_{\sigma'}\Big]$$

Auxiliary-field QMC algorithm [Hirsch, Fye (1986)]

Green function G in imaginary time (fermionic Grassmann variables ψ, ψ^*):

$$G_\sigma(\tau_2 - \tau_1) = \frac{1}{\mathcal{Z}} \int \mathcal{D}[\psi]\,\mathcal{D}[\psi^*]\;\; \psi_\sigma(\tau_1)\psi^*_\sigma(\tau_2)\;\exp\Big[\mathcal{A}_0 - U \sum_{\sigma\sigma'} \int_0^\beta d\tau\, \psi^*_\sigma \psi_\sigma \psi^*_{\sigma'} \psi_{\sigma'}\Big]$$

(i) Imaginary-time discretization $\beta = \Lambda\,\Delta\tau$

(ii) Trotter decoupling $e^{-\beta(\hat{T}+\hat{V})} \approx \left[e^{-\Delta\tau\hat{T}} e^{-\Delta\tau\hat{V}}\right]^\Lambda$

Auxiliary-field QMC algorithm [Hirsch, Fye (1986)]

Green function G in imaginary time (fermionic Grassmann variables ψ, ψ^*):

$$G_\sigma(\tau_2 - \tau_1) = \frac{1}{\mathcal{Z}} \int \mathcal{D}[\psi]\,\mathcal{D}[\psi^*]\;\; \psi_\sigma(\tau_1)\psi^*_\sigma(\tau_2)\;\; \exp\Big[\mathcal{A}_0 - U \sum_{\sigma\sigma'} \int_0^\beta d\tau\, \psi^*_\sigma \psi_\sigma \psi^*_{\sigma'} \psi_{\sigma'}\Big]$$

(i) Imaginary-time discretization $\beta = \Lambda\,\Delta\tau$

(ii) Trotter decoupling $e^{-\beta(\hat{T}+\hat{V})} \approx \big[e^{-\Delta\tau \hat{T}} e^{-\Delta\tau \hat{V}}\big]^\Lambda$

(iii) Hubbard-Stratonovich transformation

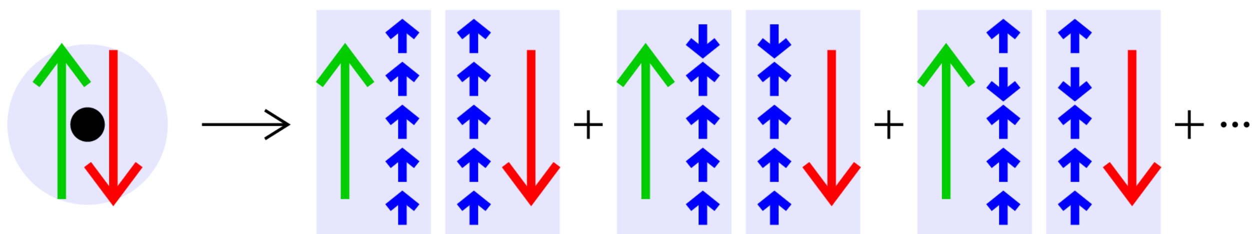

Wick theorem:

$$G = \frac{\sum M \det\{M\}}{\sum \det\{M\}}$$

Auxiliary-field QMC algorithm [Hirsch, Fye (1986)]

Green function G in imaginary time (fermionic Grassmann variables ψ, ψ^*):

$$G_\sigma(\tau_2 - \tau_1) = \frac{1}{\mathcal{Z}} \int \mathcal{D}[\psi]\,\mathcal{D}[\psi^*]\;\; \psi_\sigma(\tau_1)\psi^*_\sigma(\tau_2)\;\; \exp\Big[\mathcal{A}_0 - U \sum_{\sigma\sigma'} \int_0^\beta d\tau\, \psi^*_\sigma \psi_\sigma \psi^*_{\sigma'} \psi_{\sigma'}\Big]$$

(i) Imaginary-time discretization $\beta = \Lambda\,\Delta\tau$

(ii) Trotter decoupling $e^{-\beta(\hat{T}+\hat{V})} \approx \left[e^{-\Delta\tau \hat{T}} e^{-\Delta\tau \hat{V}}\right]^\Lambda$

(iii) Hubbard-Stratonovich transformation

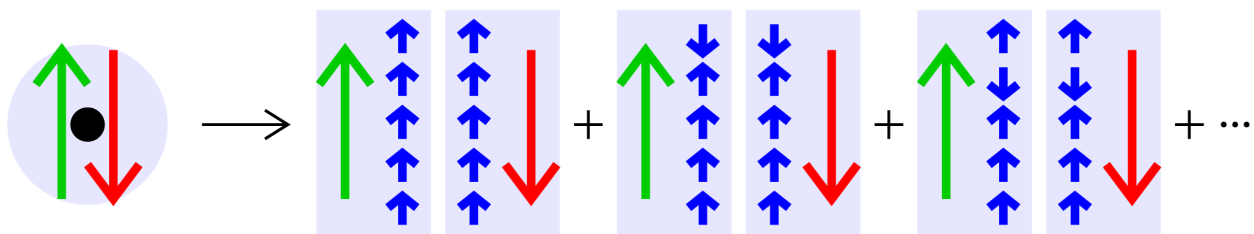

Wick theorem:

$$G = \frac{\sum M \det\{M\}}{\sum \det\{M\}}$$

(iv) MC importance sampling over auxiliary Ising field $\{s\}$: 2^Λ configurations

+ numerically exact, + no sign problem, (density-type interactions) − effort scales as T^{-3}

Multigrid Hirsch-Fye quantum Monte Carlo algorithm

State of the art: (a) conventional HF-QMC

(b) *a posteriori* extrapolation of selected observables

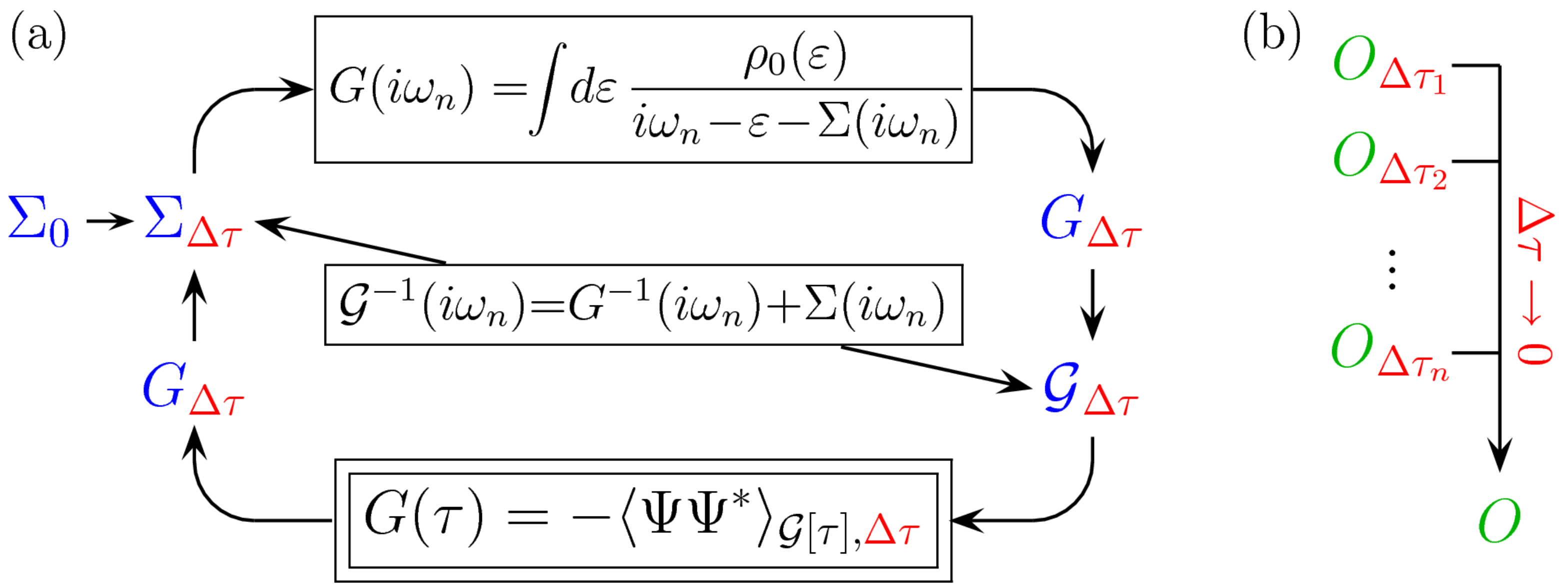

Multigrid Hirsch-Fye quantum Monte Carlo algorithm

State of the art: (a) conventional HF-QMC

(b) *a posteriori* extrapolation of selected observables

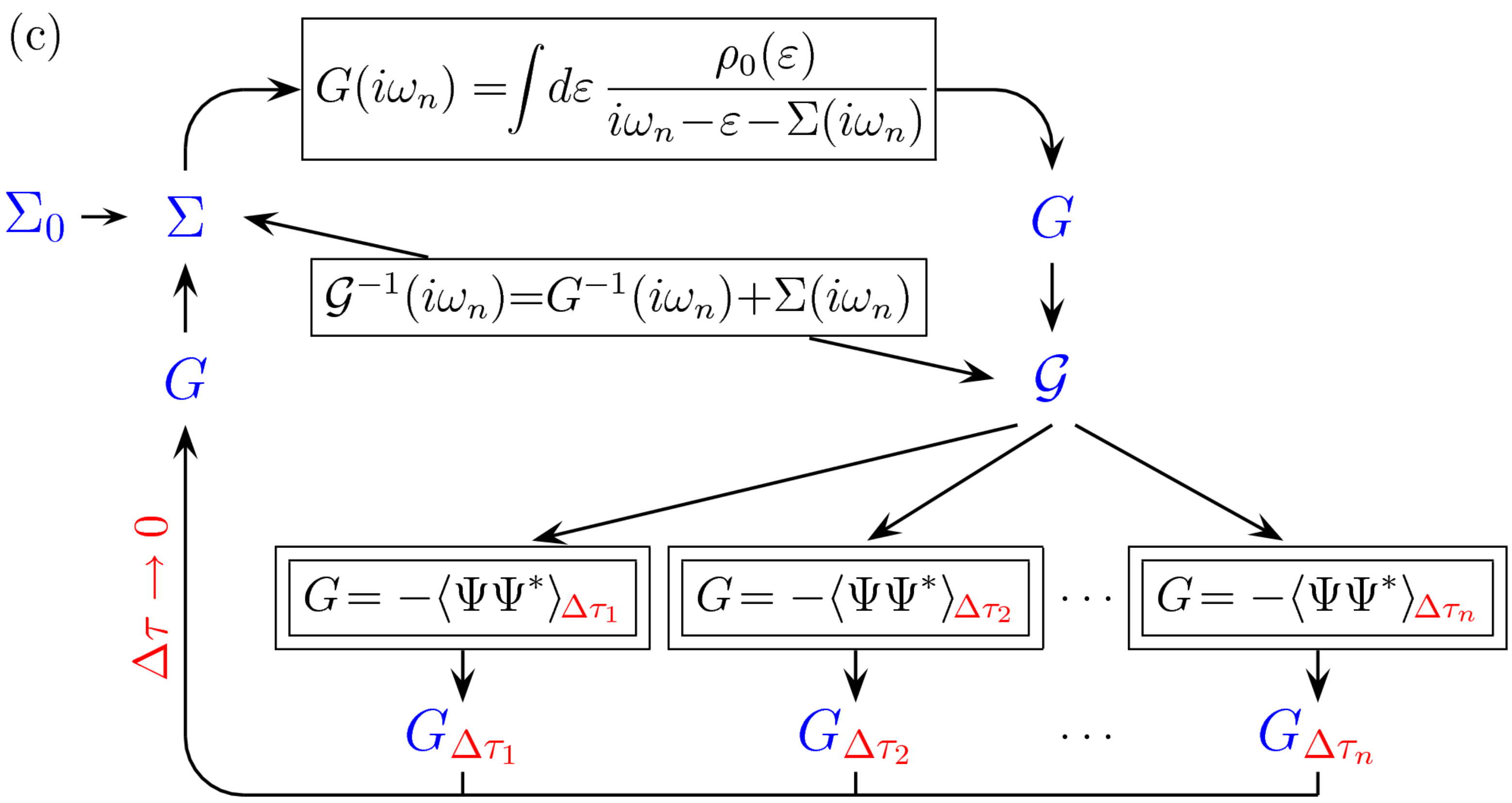

(c) Multigrid HF-QMC: internal elimination of Trotter error

$\rightsquigarrow$ quasi continuous time algorithm [NB, arXiv:0801.1222]

Schematic comparison via generalized Ginzburg-Landau functionals

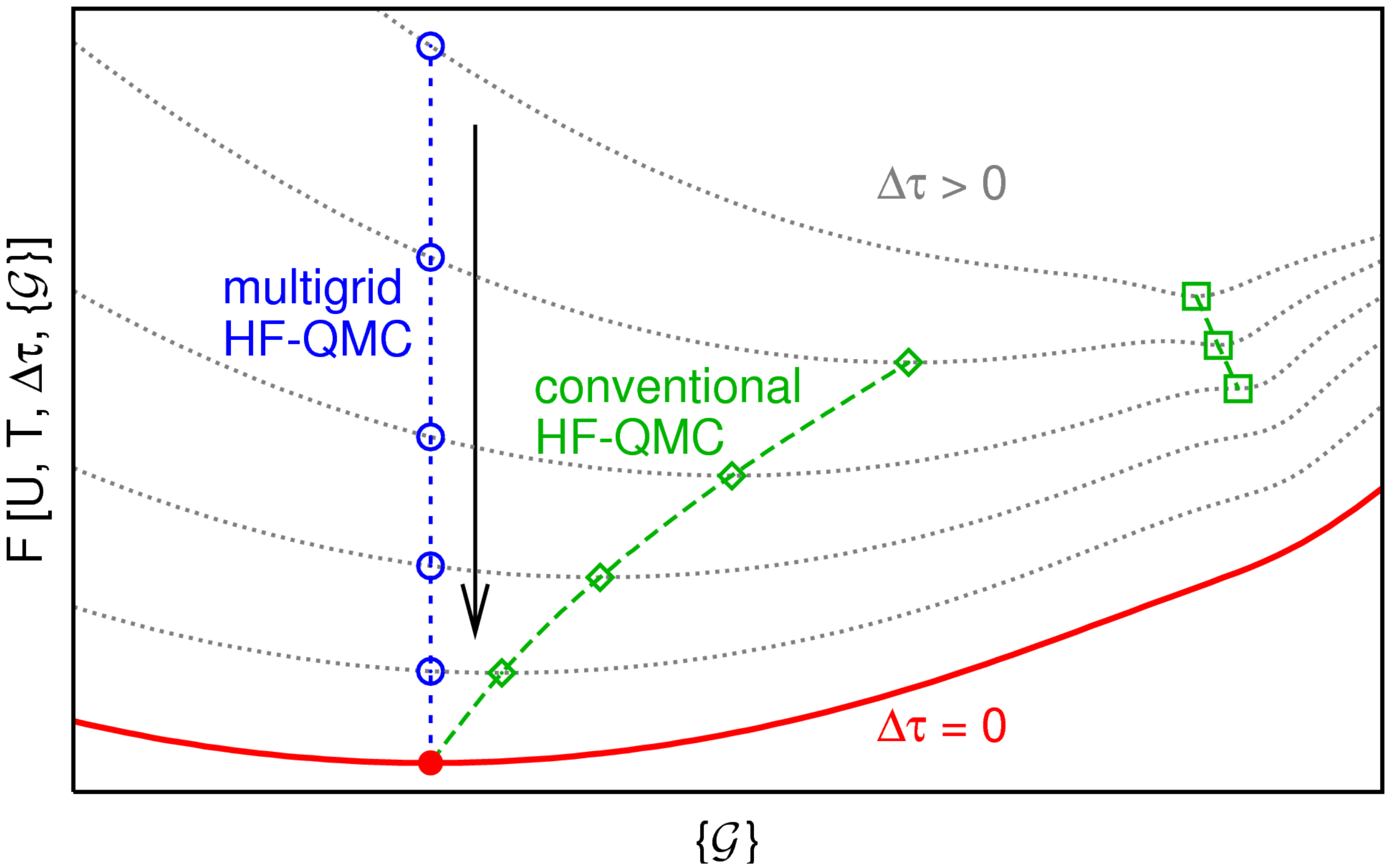

Conventional Hirsch-Fye QMC: DMFT fixed point shifts with $\Delta\tau$

Multigrid Hirsch-Fye QMC: DMFT iteration towards exact fixed point

Implementation: Green function extrapolation, hierarchy of frequency scales, . . .

Comparison: double occupancy $D = \langle n_{i\uparrow} n_{i\downarrow} \rangle$ near Mott transition

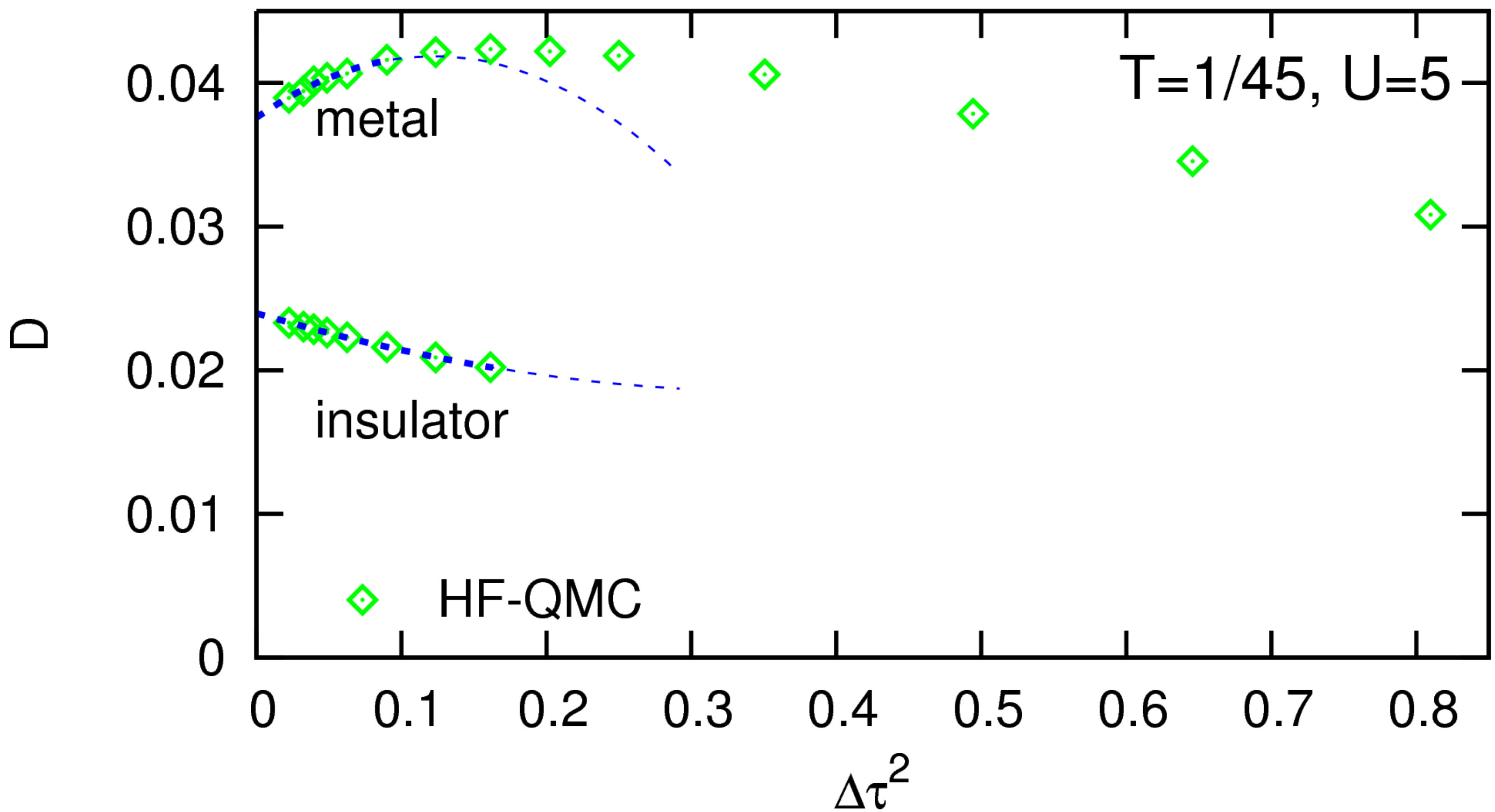

Conventional HF-QMC: no insulating solution for $\Delta\tau \gtrsim 0.4$

very irregular $\Delta\tau$ dependence beyond $\Delta\tau \approx 0.3$

Comparison: double occupancy $D = \langle n_{i\uparrow} n_{i\downarrow} \rangle$ near Mott transition

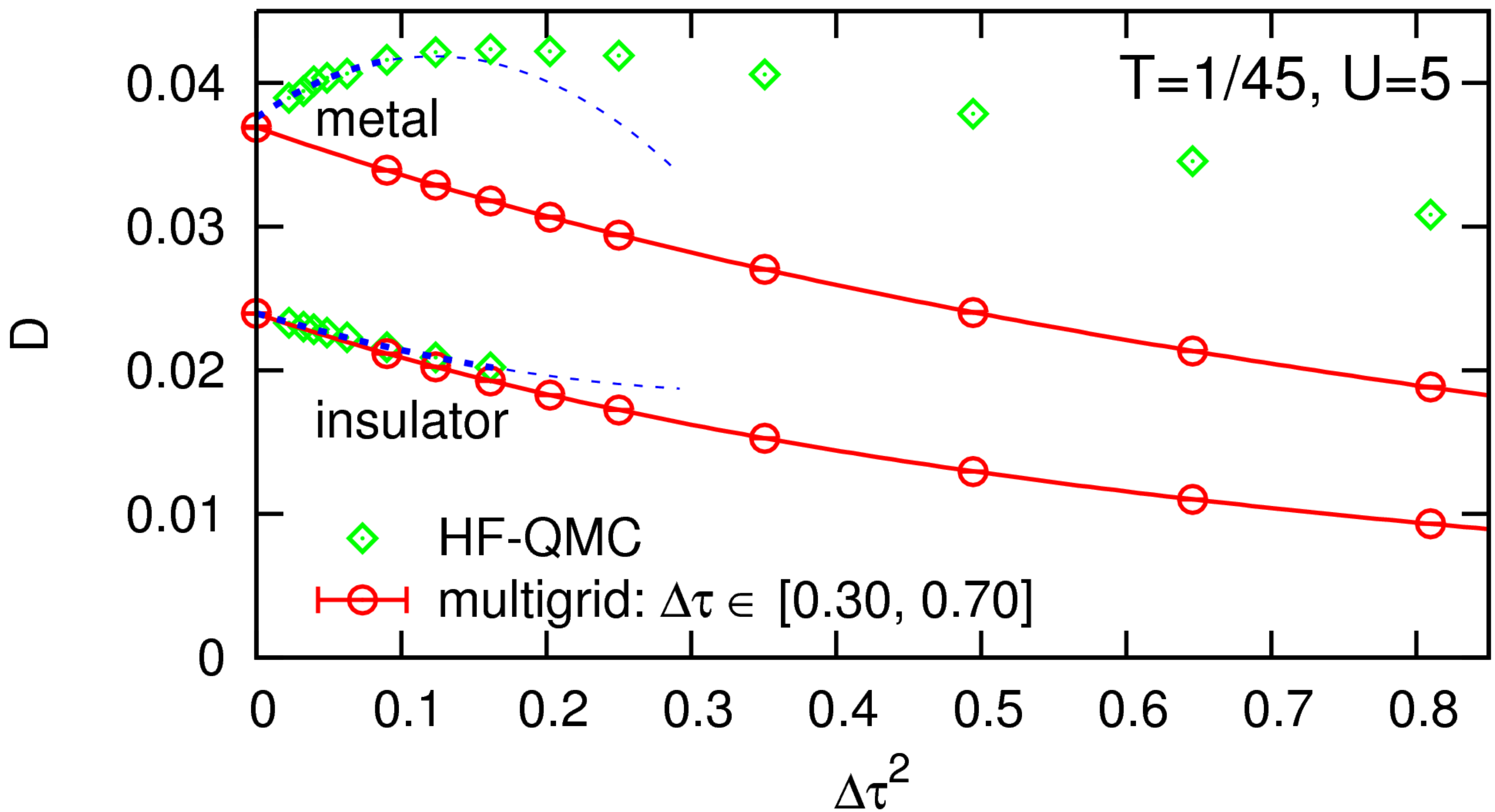

Conventional HF-QMC: no insulating solution for $\Delta\tau \gtrsim 0.4$

very irregular $\Delta\tau$ dependence beyond $\Delta\tau \approx 0.3$

Multigrid HF-QMC: vastly larger useful range of $\Delta\tau$

Systematic study: impact of grid range $[\Delta\tau_{\min}, \Delta\tau_{\max}]$

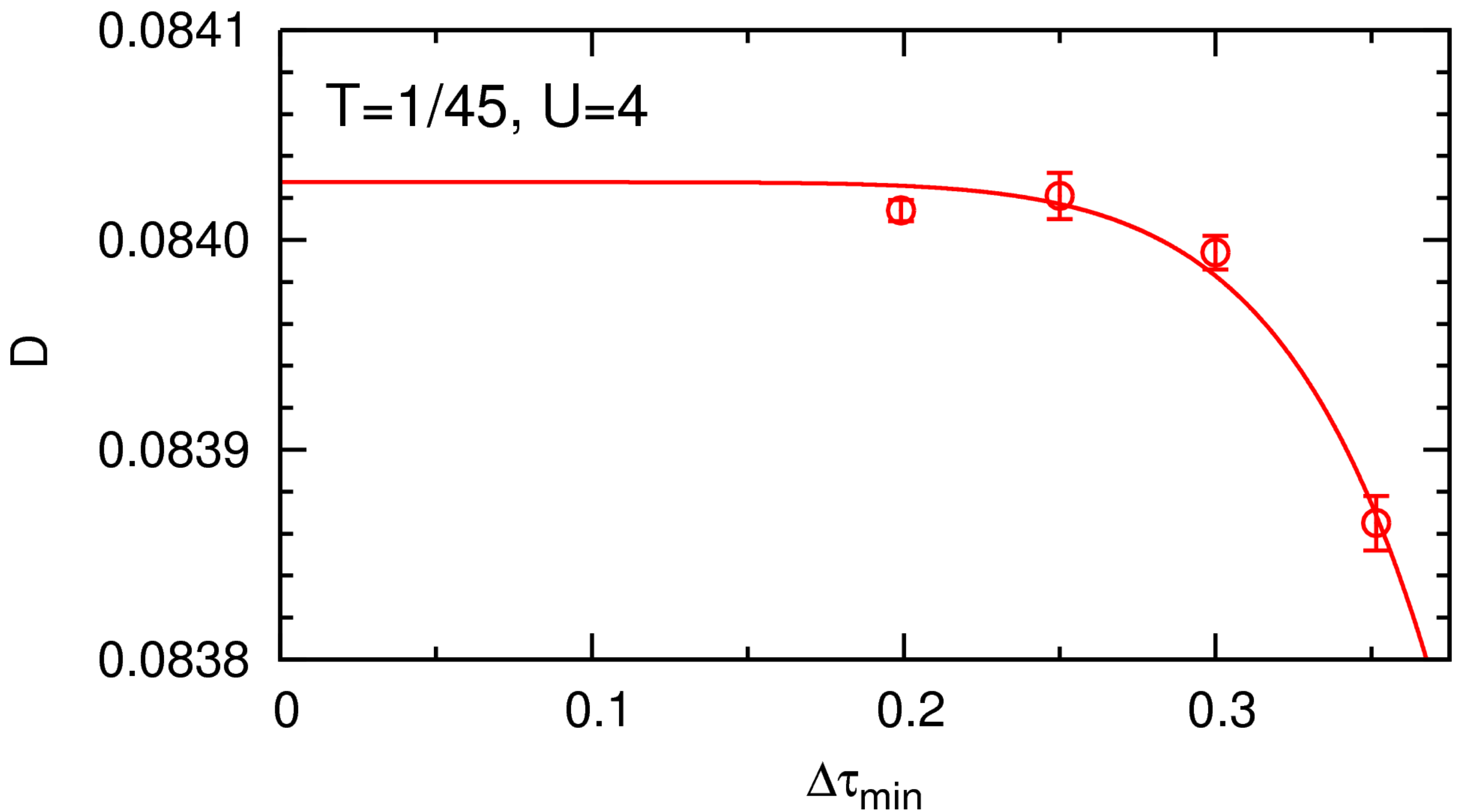

Multigrid HF-QMC usually "numerically exact" for $\tau_{\min} \lesssim 0.3$

Many successful applications: spectra, high-precision c_v, 8-band calculations, . . .

Ultracold fermions on optical lattices: model systems for strongly correlated materials

Ultracold atoms are much simpler:

Ultracold fermions on optical lattices: model systems for strongly correlated materials

Ultracold atoms are much simpler:

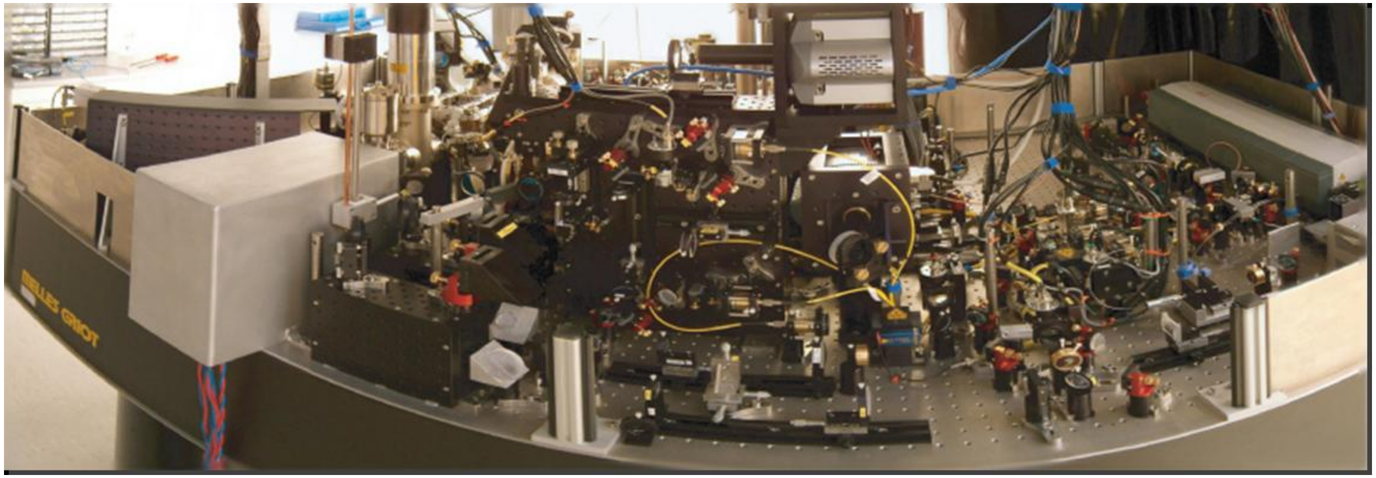

[Photo courtesy of U. Schneider]

Ultracold fermions on optical lattices: model systems for strongly correlated materials

Ultracold atoms are much simpler: 1-band assumption is often accurate

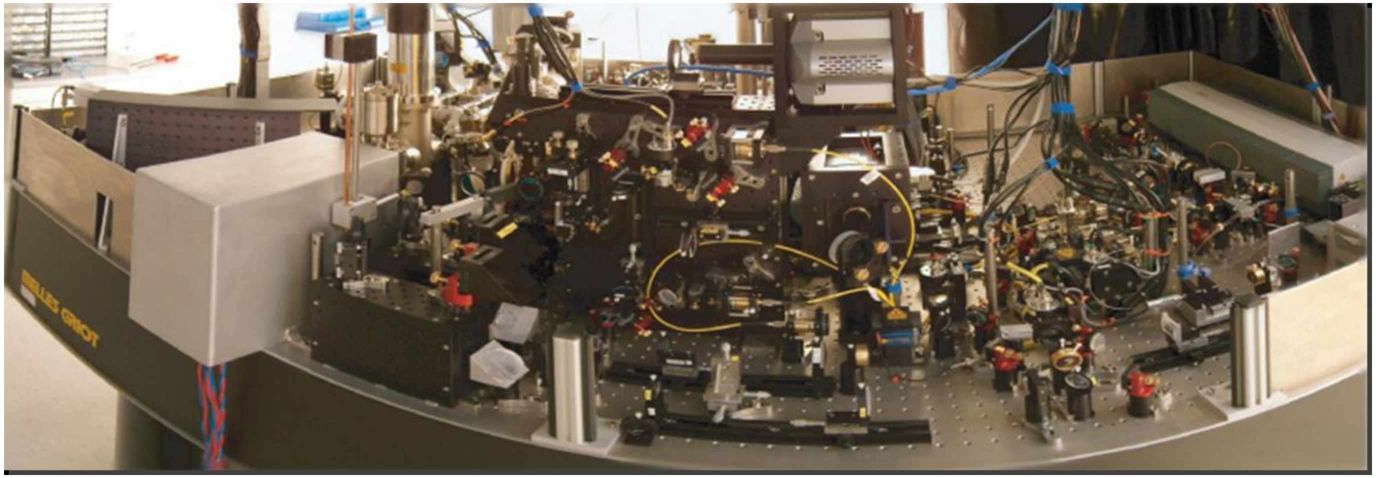

[Photo courtesy of U. Schneider]

Ultracold fermions on optical lattices: model systems for strongly correlated materials

Ultracold atoms are much simpler: 1-band assumption is often accurate

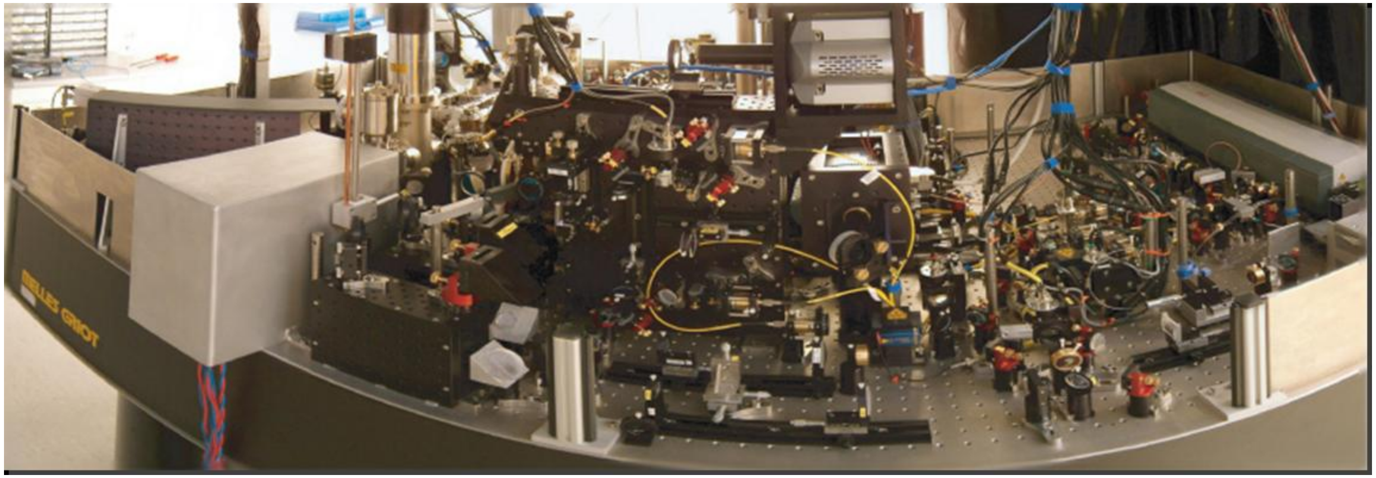

[Photo courtesy of U. Schneider]

But: trapping potential $\rightsquigarrow$ inhomogeneous systems

finite cloud sizes

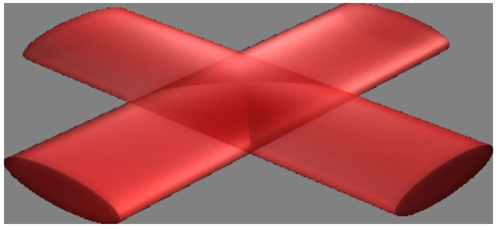

Ultracold fermions on optical lattices: model systems for strongly correlated materials

Ultracold atoms are much simpler: 1-band assumption is often accurate

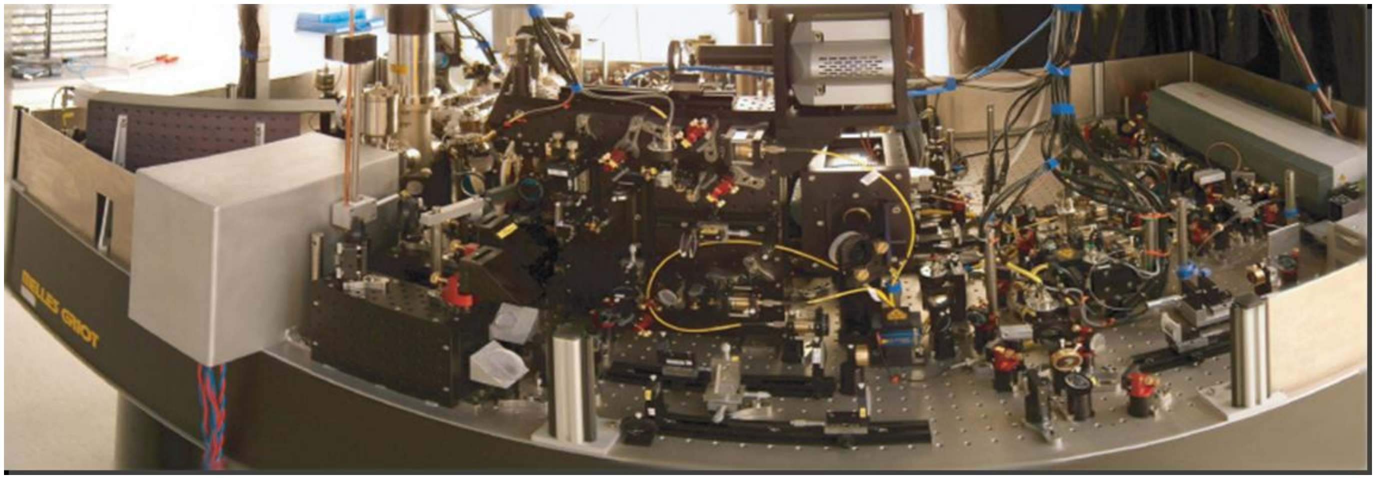

[Photo courtesy of U. Schneider]

But: trapping potential $\rightsquigarrow$ inhomogeneous systems

finite cloud sizes

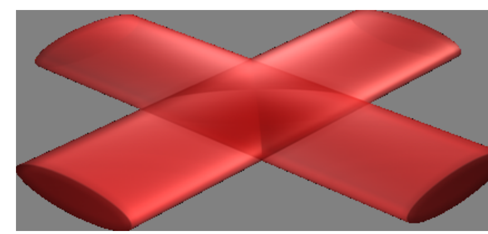

Note: more possibilities, e.g. 3-flavor systems

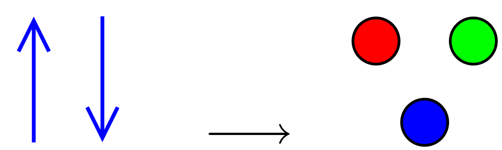

Paramagnetic Mott transitions in 3-flavor mixtures

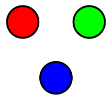

3 flavors: simplest case beyond electronic systems
1st approximation: all flavors equivalent

Paramagnetic Mott transitions in 3-flavor mixtures

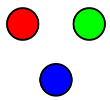

3 flavors: simplest case beyond electronic systems
1st approximation: all flavors equivalent

- Qualitatively new physics: $U < 0$, $n = 1.5$ [Hofstetter, PRB (2004), PRL (2007)]

  Color superconductivity
  Trionic phase
  . . .

Paramagnetic Mott transitions in 3-flavor mixtures

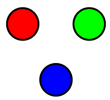

3 flavors: simplest case beyond electronic systems

1st approximation: all flavors equivalent

- Qualitatively new physics: $U < 0$, $n = 1.5$ [Hofstetter, PRB (2004), PRL (2007)]

  Color superconductivity

  Trionic phase

  . . .

- Ordered phases: $U > 0$, $n = 1$

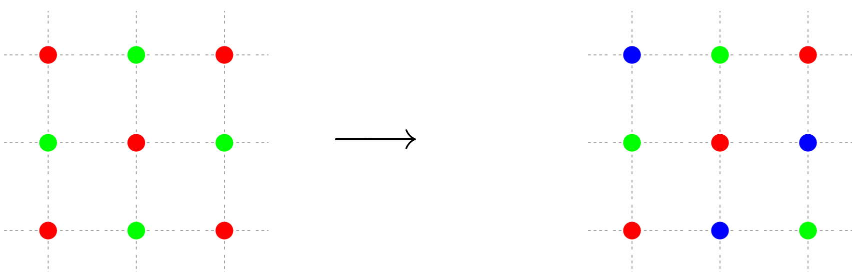

2 spins/flavors

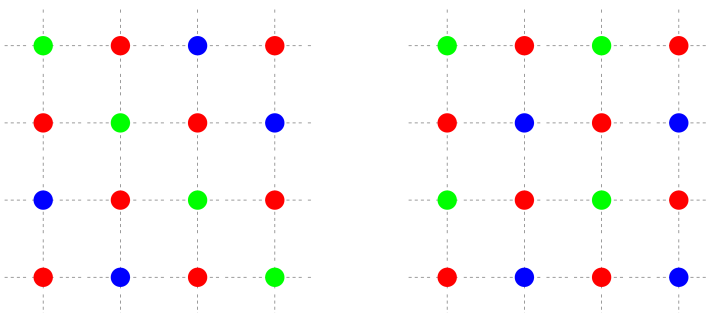

3 spins/flavors

Paramagnetic Mott transitions in 3-flavor mixtures

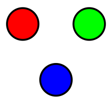

3 flavors: simplest case beyond electronic systems
1st approximation: all flavors equivalent

- Qualitatively new physics: $U < 0$, $n = 1.5$ [Hofstetter, PRB (2004), PRL (2007)]

  Color superconductivity
  Trionic phase
  . . .

- Ordered phases: $U > 0$, $n = 1$

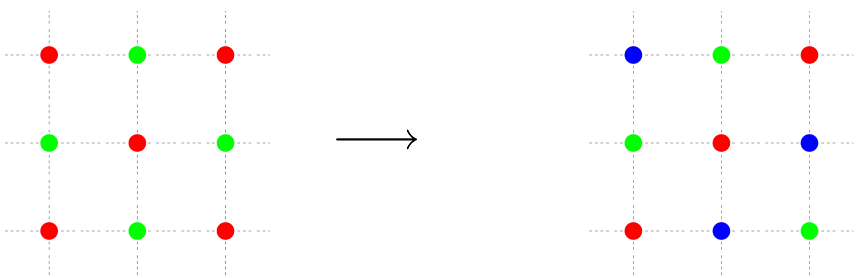

2 spins/flavors

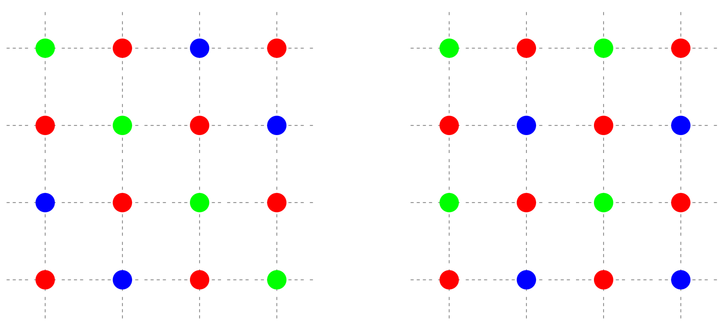

3 spins/flavors

Most "electron-like": $U > 0$, paramagnetic phase

Results at low T: particle density n and compressibility $\kappa = \frac{dn}{d\mu}$ (vs. μ)

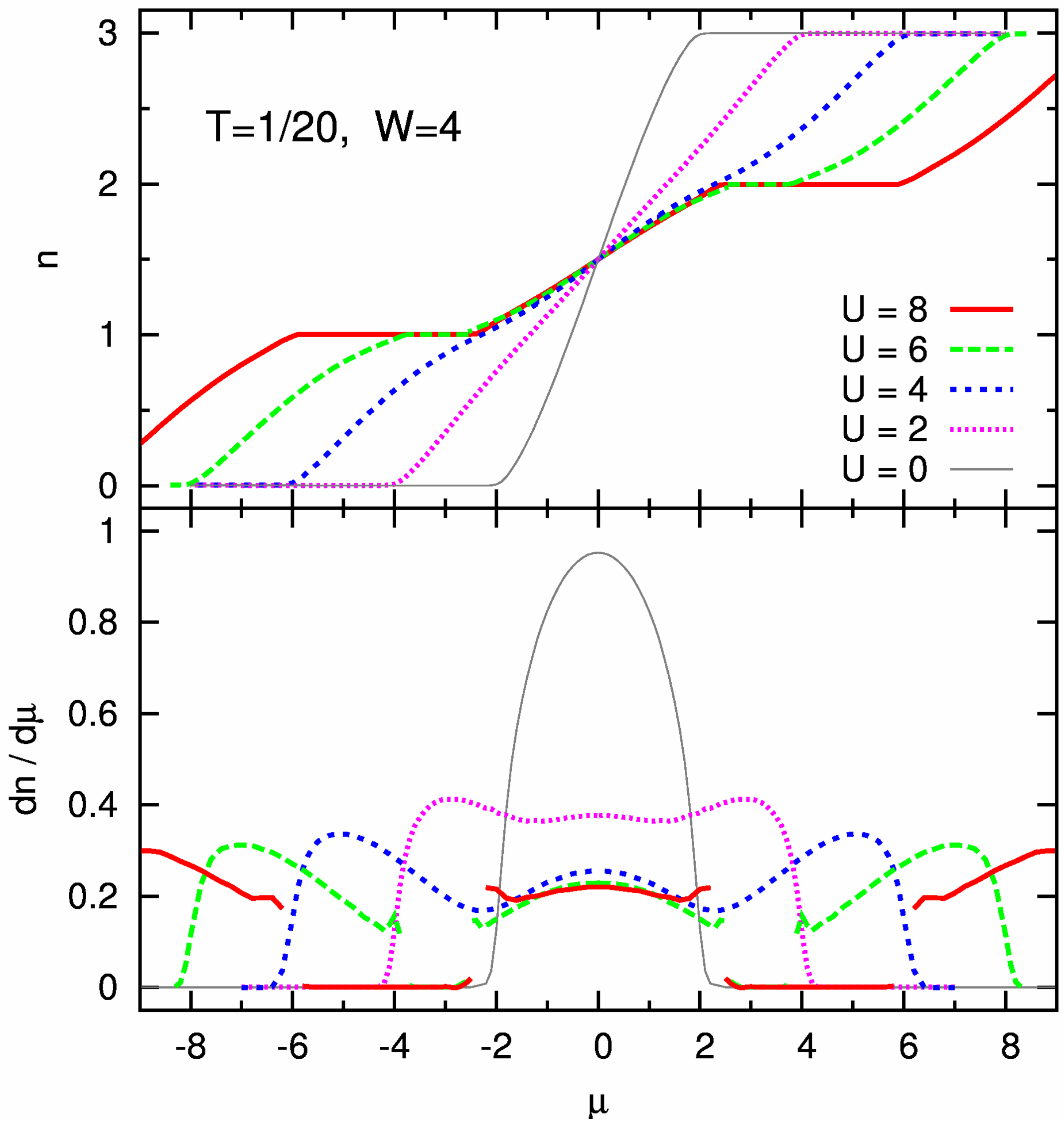

HF-QMC, Bethe DOS ($W = 4$)

Plateaus at integer filling ($U \gtrsim 5.5$)

$\rightsquigarrow$ incompressible Mott phases

[E. Gorelik, N. Blümer, arXiv:0904.4610]

Results at low T: particle density n and compressibility $\kappa = \frac{dn}{d\mu}$ (vs. μ)

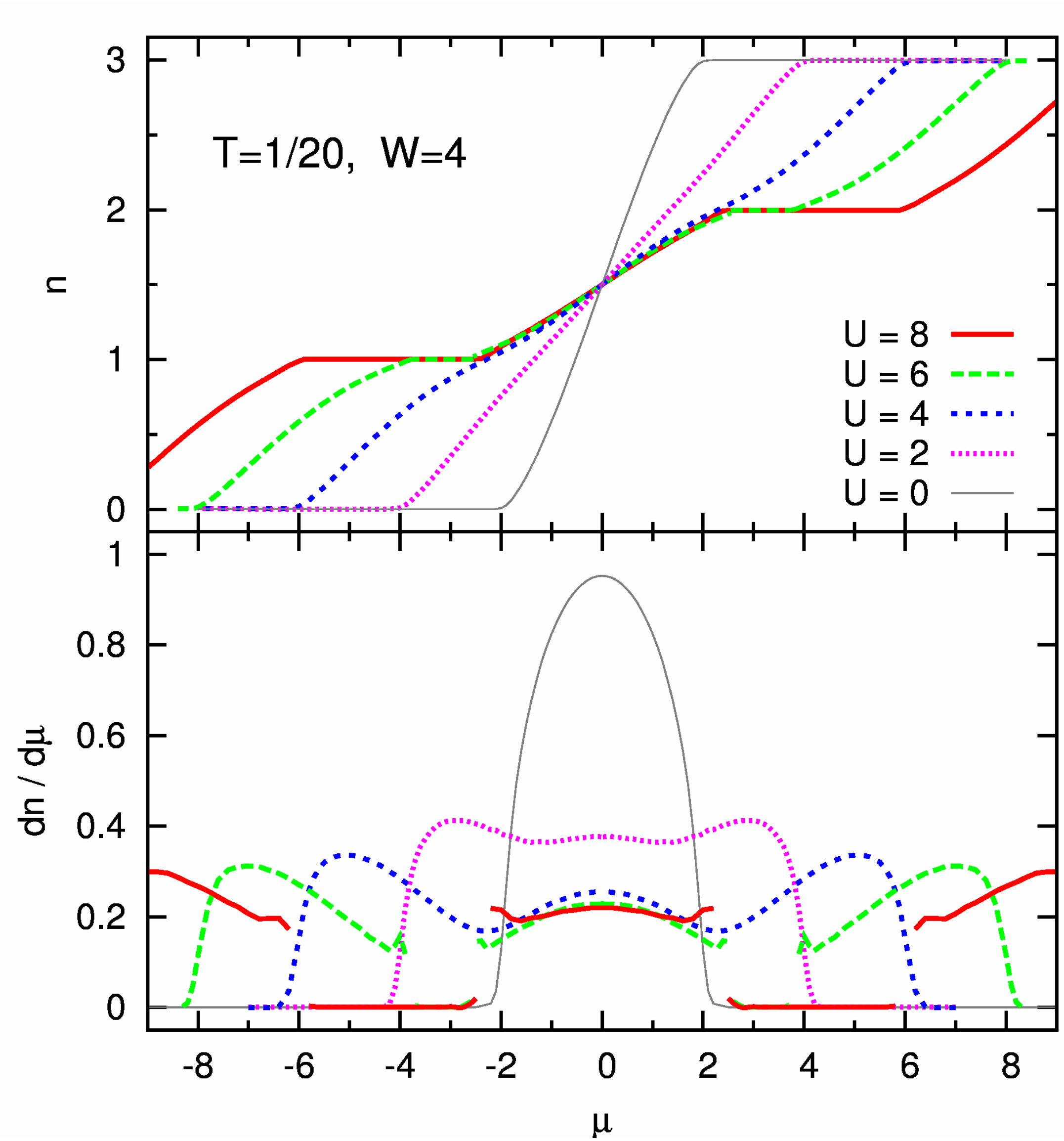

HF-QMC, Bethe DOS ($W = 4$)

Plateaus at integer filling ($U \gtrsim 5.5$)

$\rightsquigarrow$ incompressible Mott phases

$1 < n < 2$: semi-compressible phase

κ independent of μ, U, T

[E. Gorelik, N. Blümer, arXiv:0904.4610]

Results at low T: particle density n and compressibility $\kappa = \frac{dn}{d\mu}$ (vs. μ)

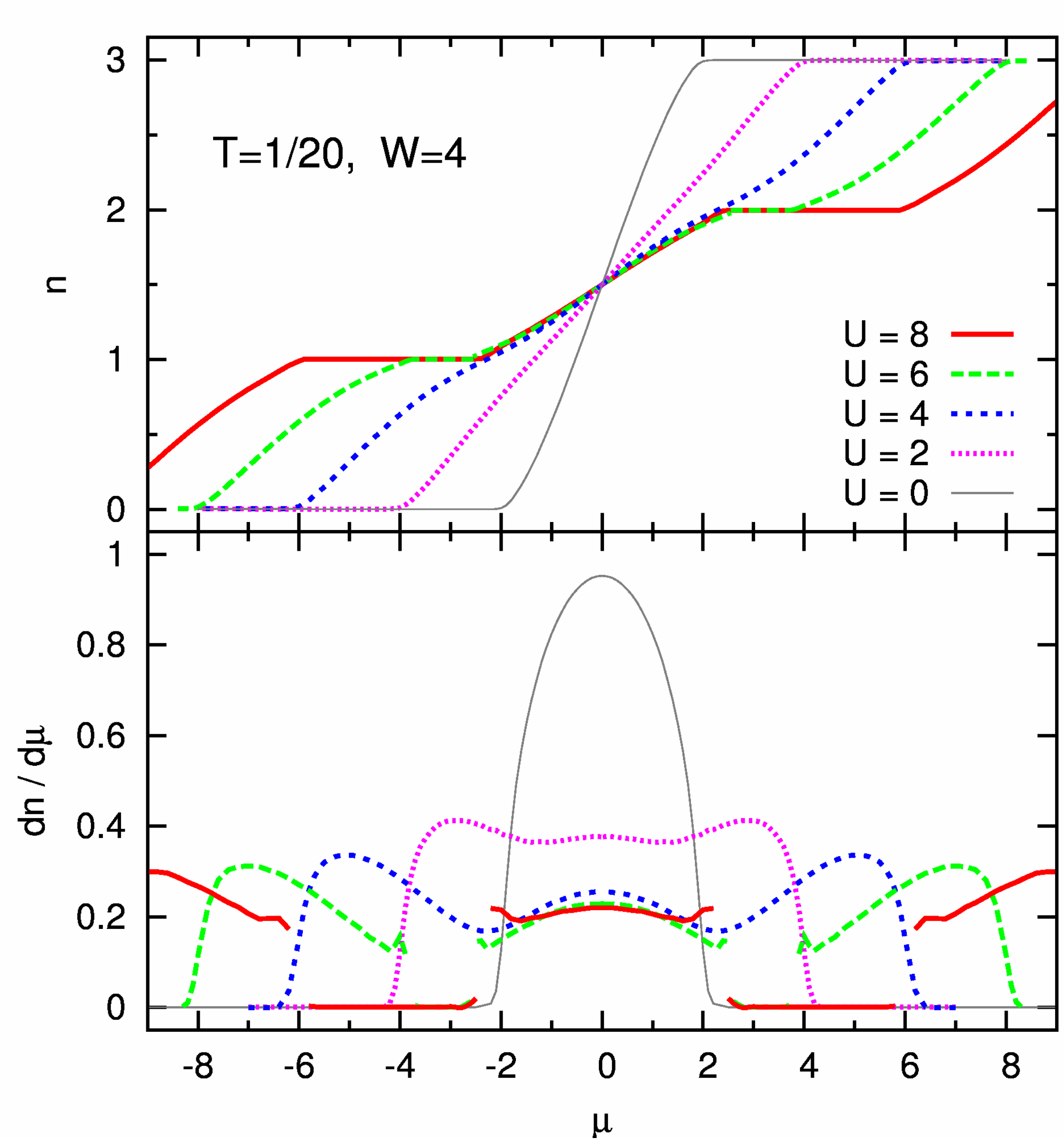

HF-QMC, Bethe DOS ($W = 4$)

Plateaus at integer filling ($U \gtrsim 5.5$)

$\rightsquigarrow$ incompressible Mott phases

$1 < n < 2$: semi-compressible phase

κ independent of μ, U, T

Contrast with SU(4) system:

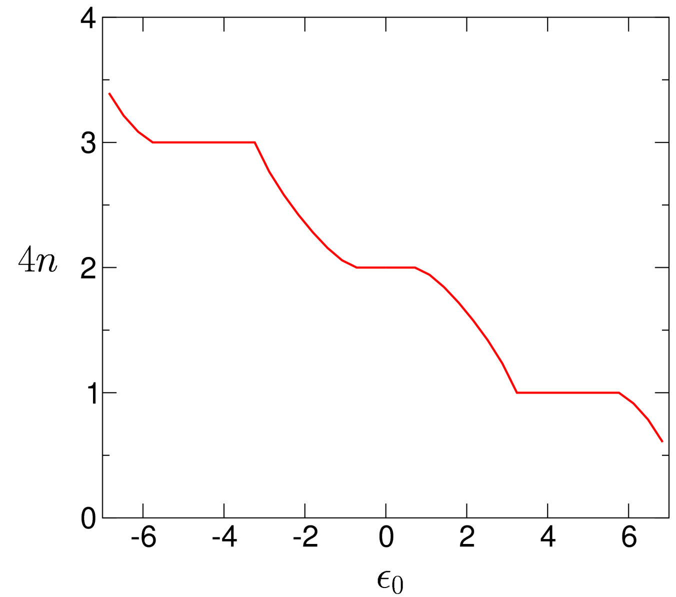

[E. Gorelik, N. Blümer, arXiv:0904.4610]

[Florens, Georges, PRB **70**, 035114 (2004)]

T dependence of density n and compressibility κ

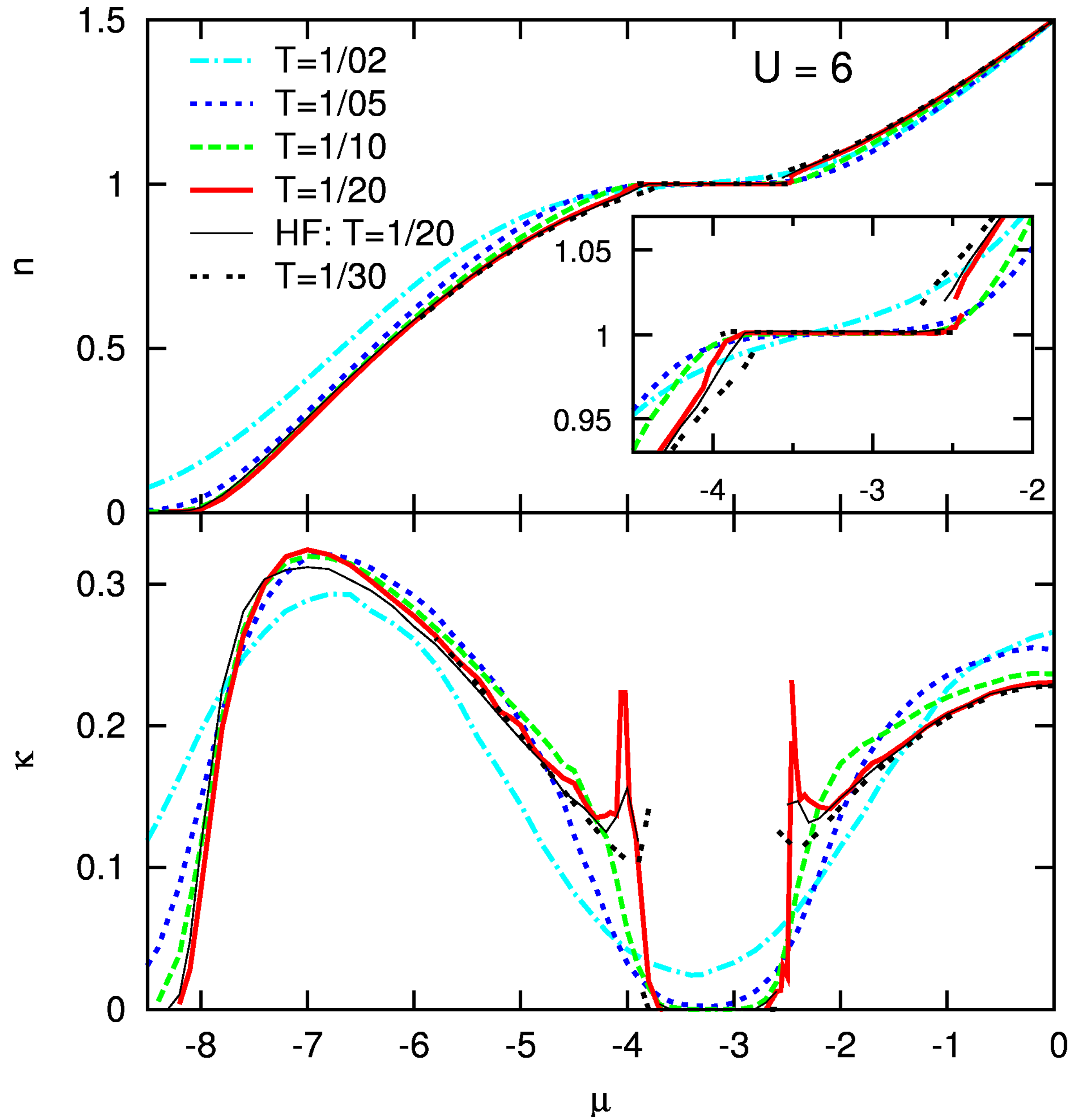

Multigrid HF-QMC results

(also HF-QMC at $T = 1/20$):

Critical temperature $T^* \approx 1/20$

T dependence of density n and compressibility κ

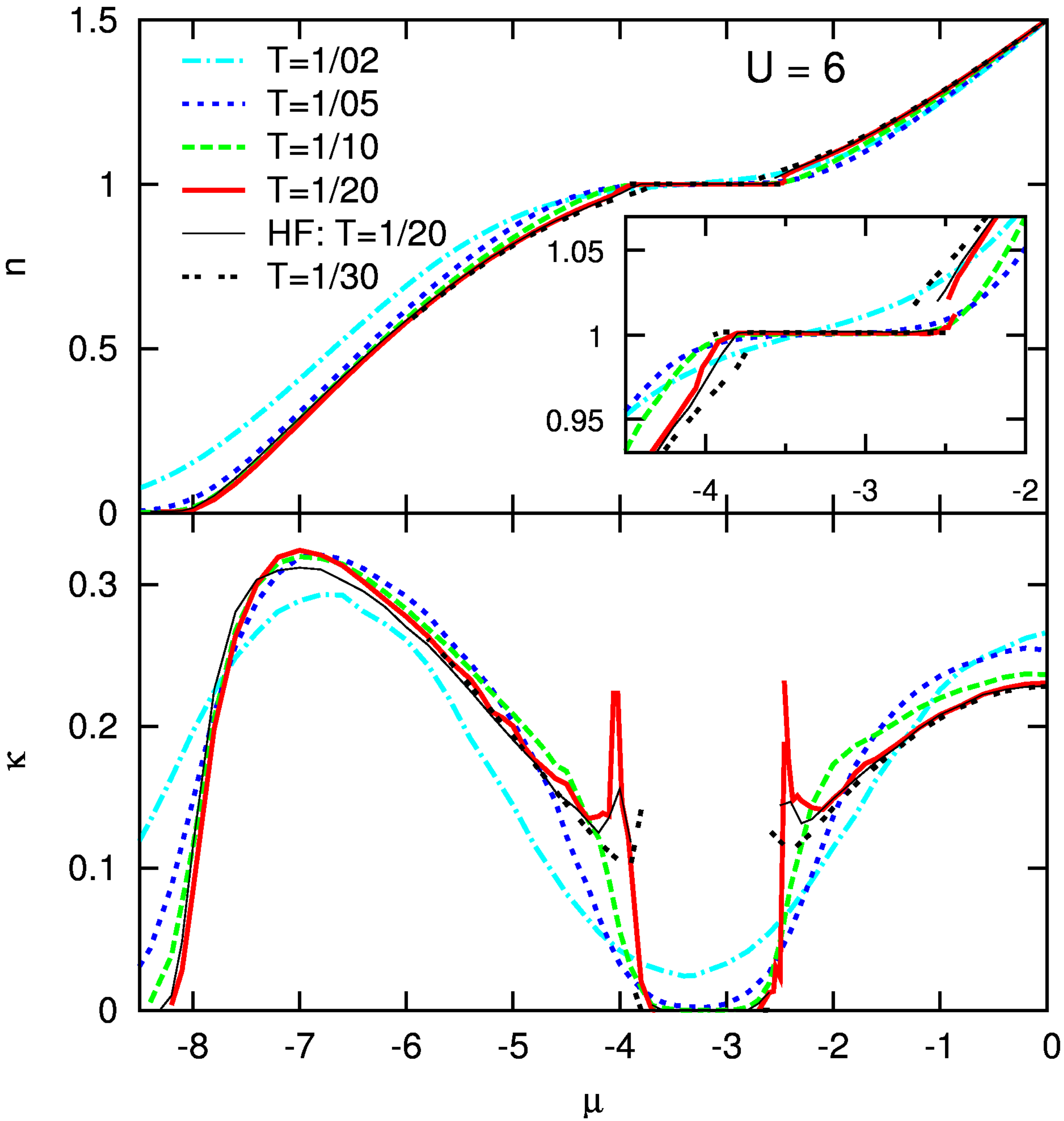

Multigrid HF-QMC results

(also HF-QMC at T = 1/20):

Critical temperature $T^* \approx 1/20$

Important for experiments:

Signatures of Mott transition persist to high temperatures:

nearly complete suppression of κ (at $n \approx 1$) up to $T \approx 1/5$.

T dependence of density n and compressibility κ

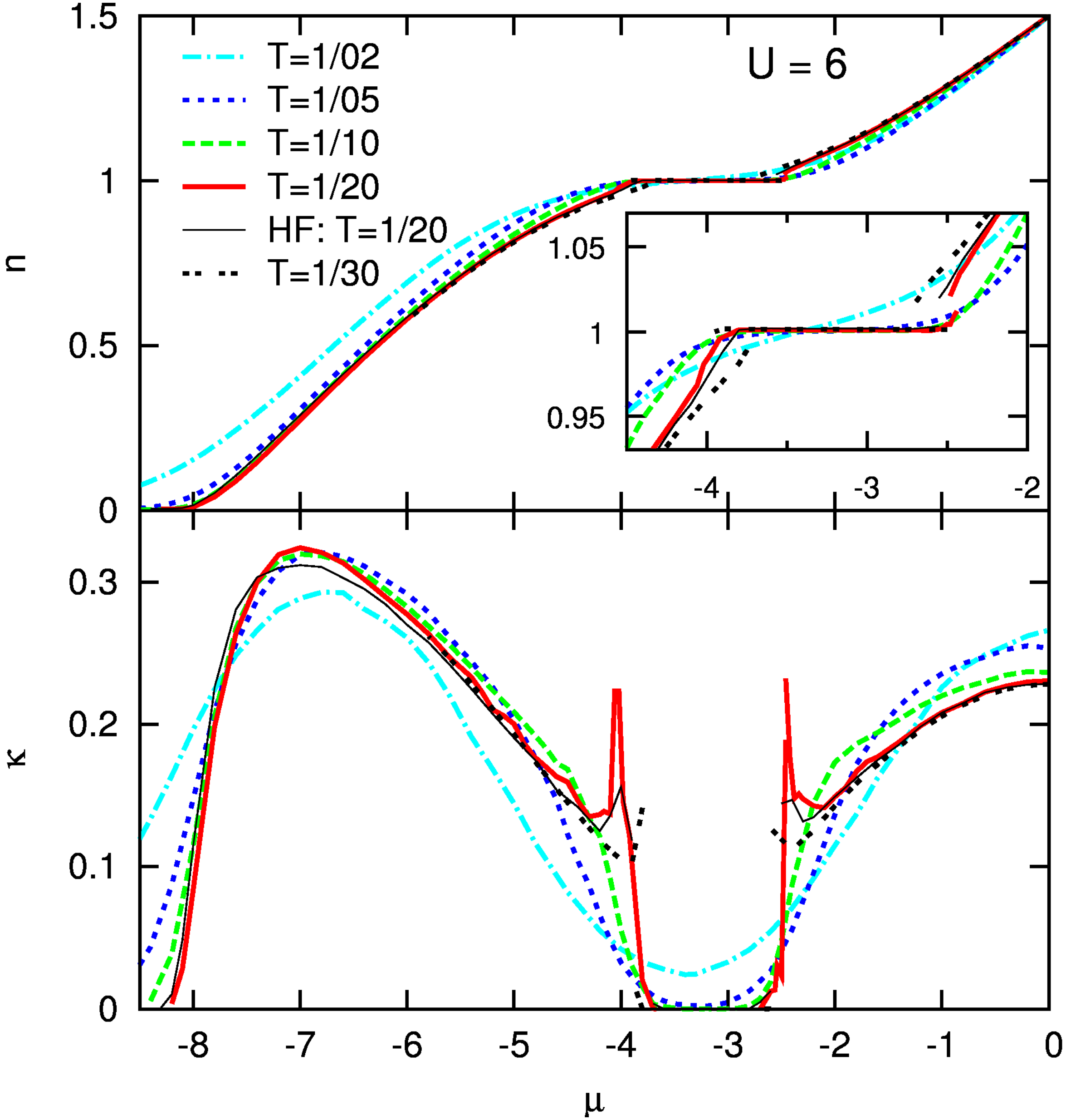

Multigrid HF-QMC results

(also HF-QMC at $T = 1/20$):

Critical temperature $T^* \approx 1/20$

Important for experiments:

Signatures of Mott transition persist to high temperatures:

nearly complete suppression of κ (at $n \approx 1$) up to $T \approx 1/5$.

skip: pair occupancy, spectra

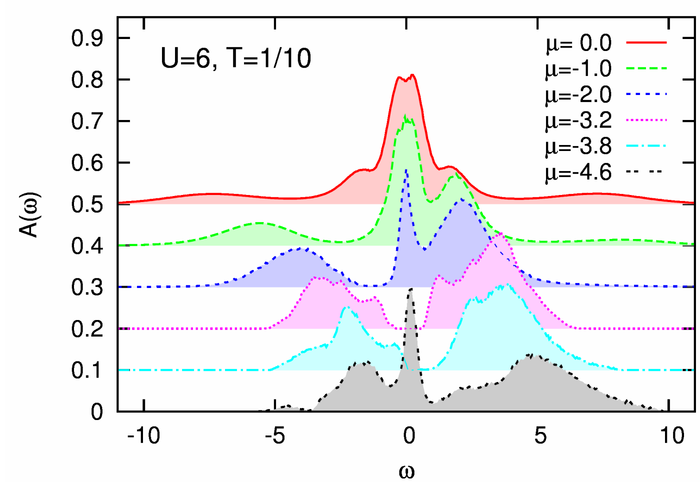

Impact of the lattice type

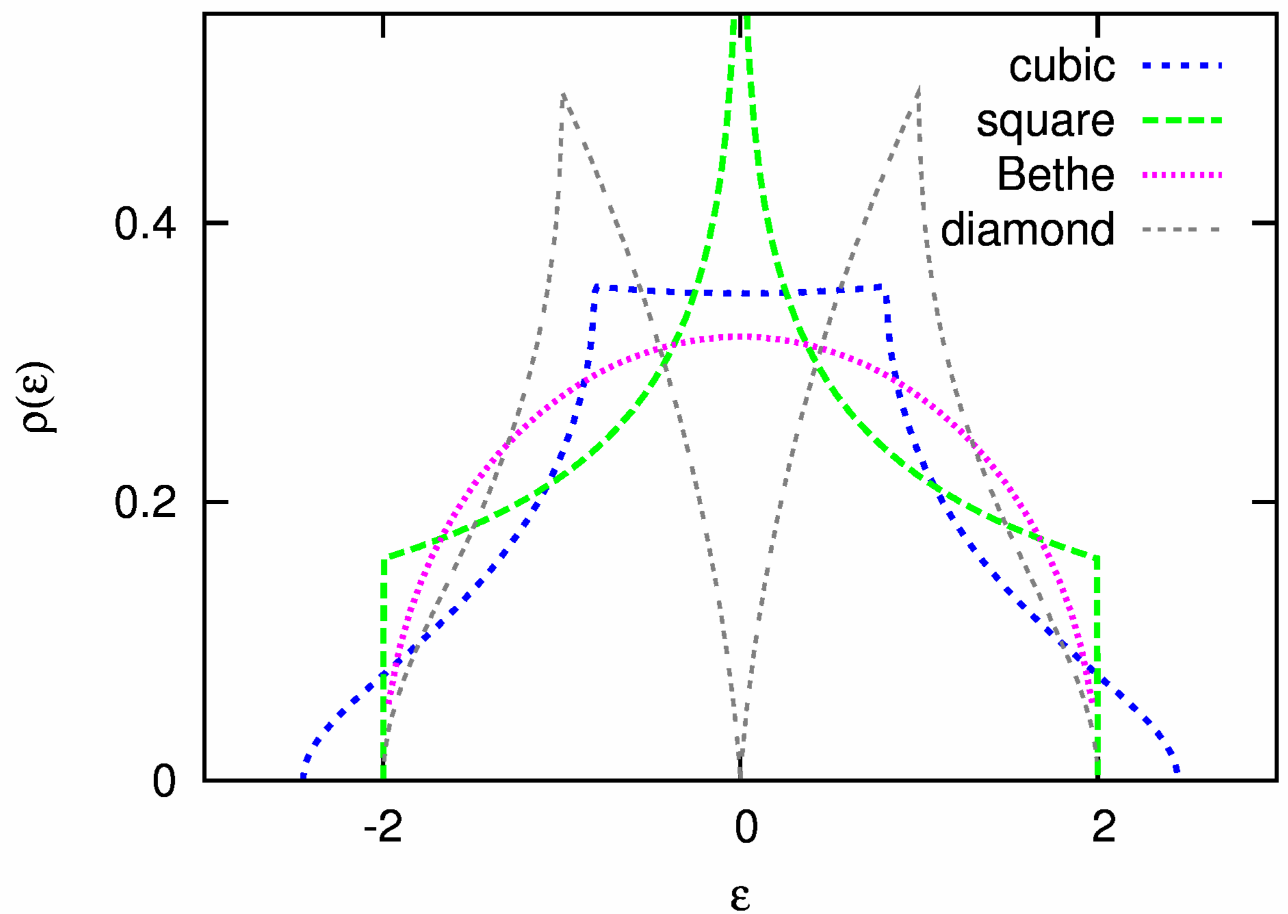

Noninteracting densities of states (variance $\int \epsilon^2 \rho(\epsilon) d\epsilon = 1$)

Question: Would DMFT results for the cubic (square) lattice differ significantly?

Dependence of filling and compressibility (vs. μ) on the lattice type

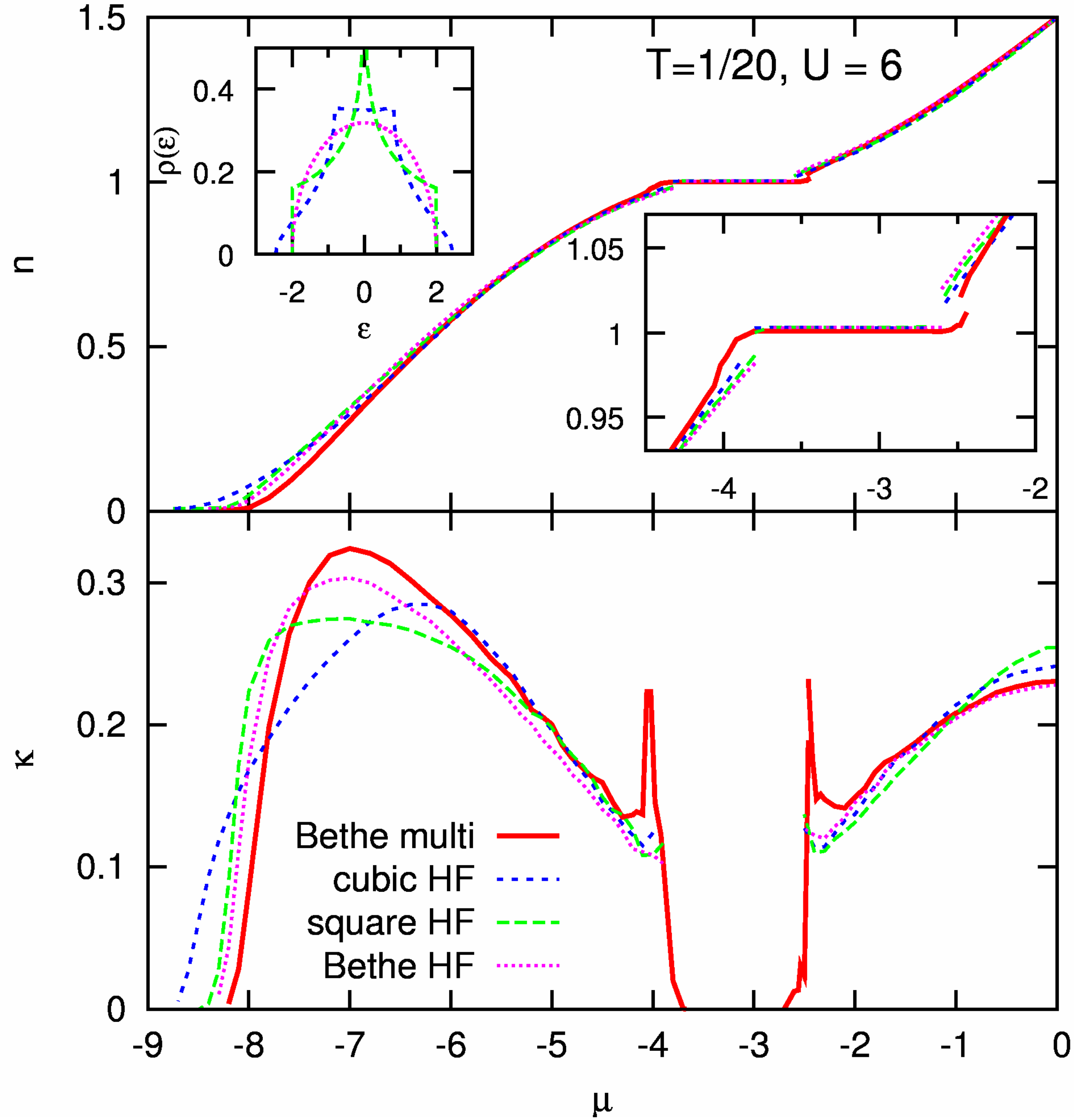

- minor differences for $n \geq 0.5$
- nearly identical gap width
- significant lattice impact only near the band edges (and at $\mu \approx 0$)
- not shown: double occupancy $D(n)$ indistinguishable

Spectral function $A(\omega)$ for different lattice types

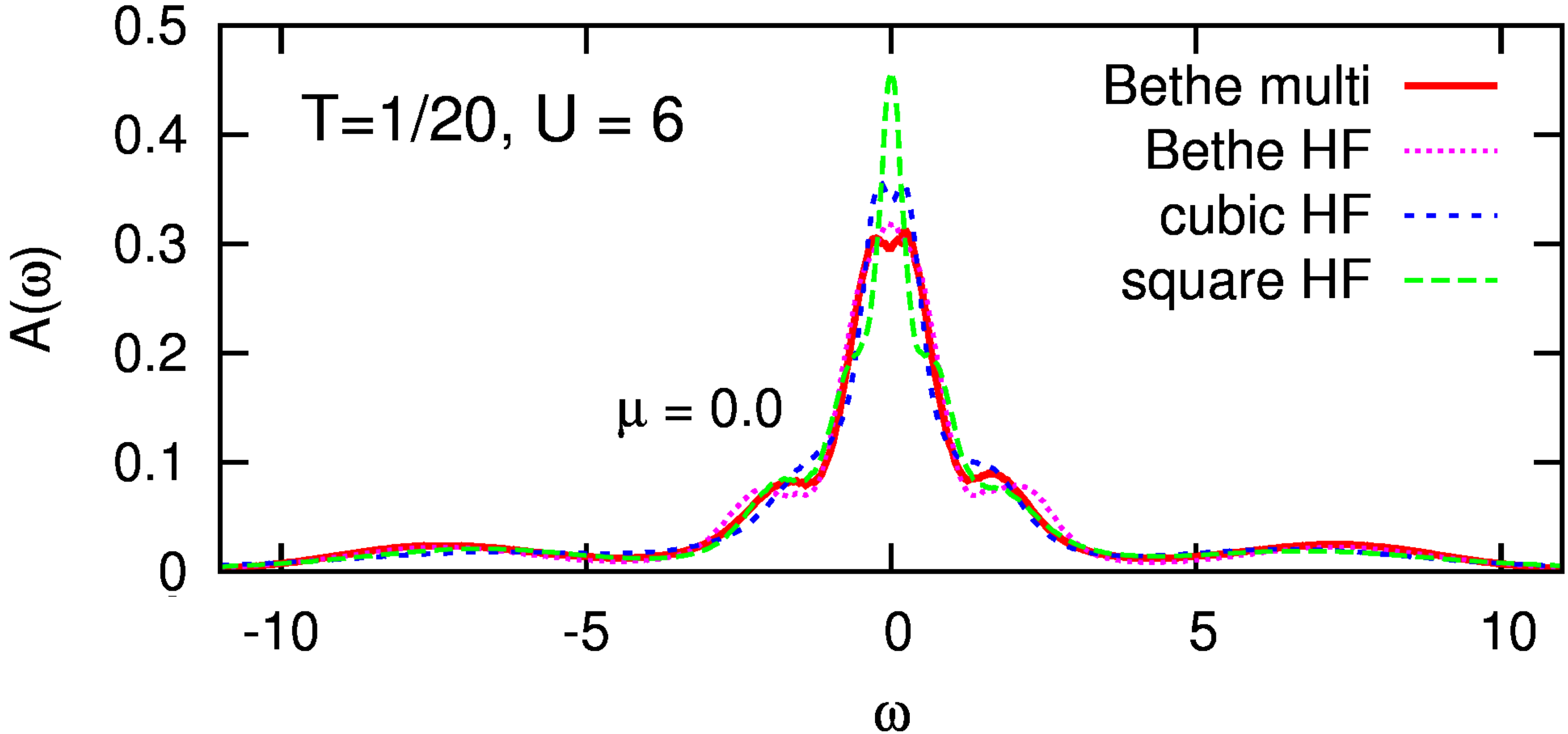

Strong lattice sensitivity at small ω in Fermi liquid regime

Melting of an antiferromagnet in an optical trap

Now include trapping potential, e.g.: $V_i = V r_i^2$

$$H = -\sum_{(ij),\sigma} t_{ij}\, c^\dagger_{i\sigma} c_{j\sigma} + U \sum_{i=1}^{N} n_{i\uparrow} n_{i\downarrow} + \sum_{i,\sigma} V_i\, n_{i\sigma}$$

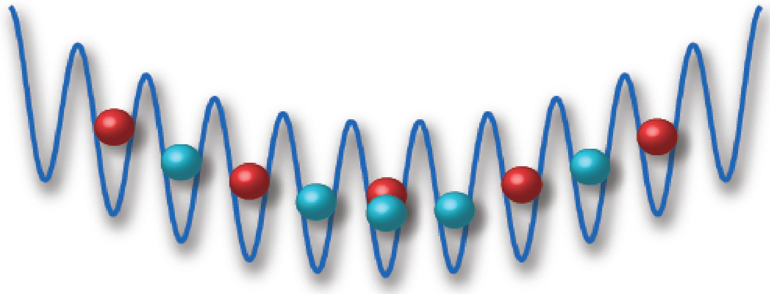

Melting of an antiferromagnet in an optical trap

Now include trapping potential, e.g.: $V_i = V r_i^2$

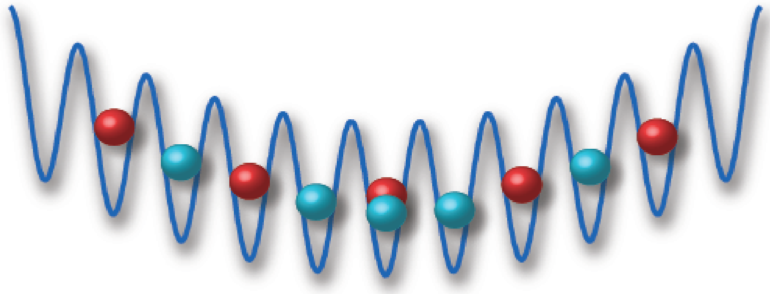

$$H = -\sum_{(ij),\sigma} t_{ij}\, c^\dagger_{i\sigma} c_{j\sigma} + U \sum_{i=1}^{N} n_{i\uparrow} n_{i\downarrow} + \sum_{i,\sigma} V_i\, n_{i\sigma}$$

Real-space DMFT: use local self-energy in inhomogeneous system

$\rightsquigarrow$ N single-site impurities, coupled by modified lattice Dyson equation:

$$\Big[G_\sigma(i\omega_n)\Big]^{-1}_{ij} = \big(\mu_\sigma + i\omega_n\big)\delta_{ij} \quad - \; t_{ij} \quad - \; \big(V_i + \Sigma_{i\sigma}(i\omega_n)\big)\delta_{ij}$$

[M. Snoek, I. Titvinidze, C. Toke, K. Byczuk, and W. Hofstetter, New Journal of Physics (2008); R. Helmes, T. A. Costi, and A. Rosch, PRL (2008)]

Also: inhomogeneous DMFT (for Falicov-Kimball model) [Freericks]

Melting of an antiferromagnet in an optical trap

Now include trapping potential, e.g.: $V_i = V r_i^2$

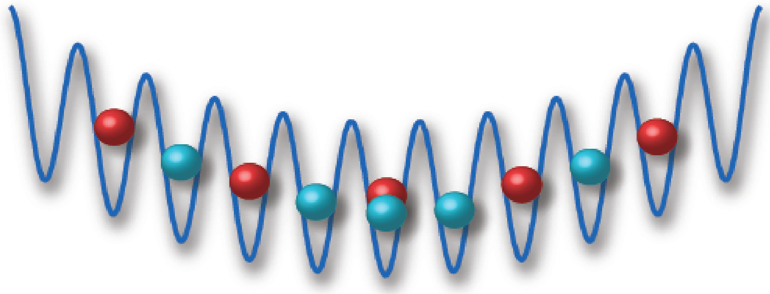

$$H = -\sum_{(ij),\sigma} t_{ij}\, c^\dagger_{i\sigma} c_{j\sigma} + U \sum_{i=1}^{N} n_{i\uparrow} n_{i\downarrow} + \sum_{i,\sigma} V_i\, n_{i\sigma}$$

Real-space DMFT: use local self-energy in inhomogeneous system

$\rightsquigarrow$ N single-site impurities, coupled by modified lattice Dyson equation:

$$\left[G_\sigma(i\omega_n)\right]^{-1}_{ij} = \left(\mu_\sigma + i\omega_n\right)\delta_{ij} - t_{ij} - \left(V_i + \Sigma_{i\sigma}(i\omega_n)\right)\delta_{ij}$$

[M. Snoek, I. Titvinidze, C. Toke, K. Byczuk, and W. Hofstetter, New Journal of Physics (2008); R. Helmes, T. A. Costi, and A. Rosch, PRL (2008)]

Also: inhomogeneous DMFT (for Falicov-Kimball model) [Freericks]

Note: impurity problem is site-parallel, lattice Dyson equation is frequency-parallel

All previous implementations: RDMFT+NRG

NRG: problematic at elevated temperatures

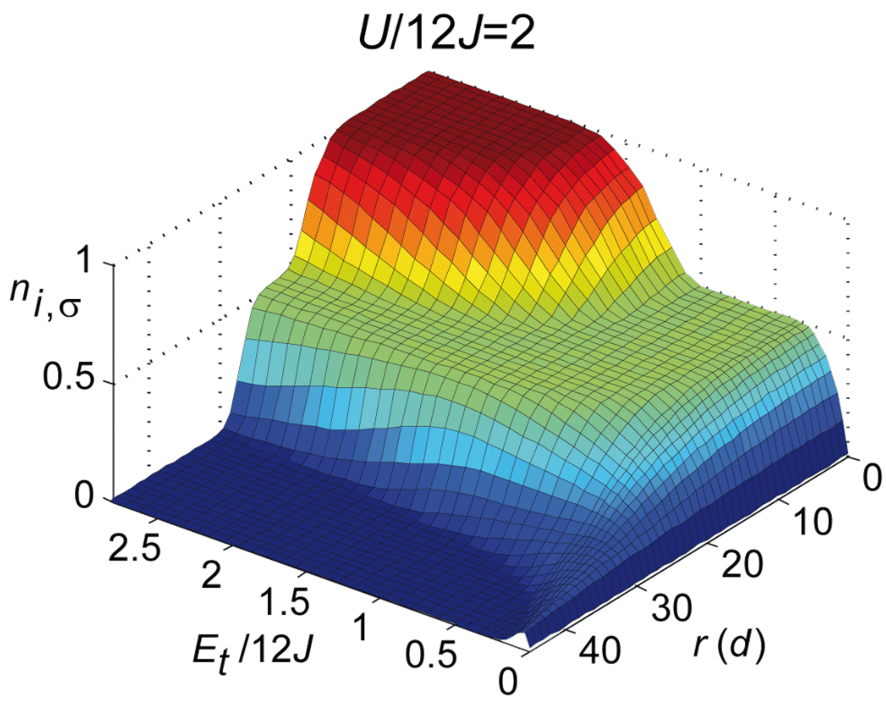

$T = 0.07t$

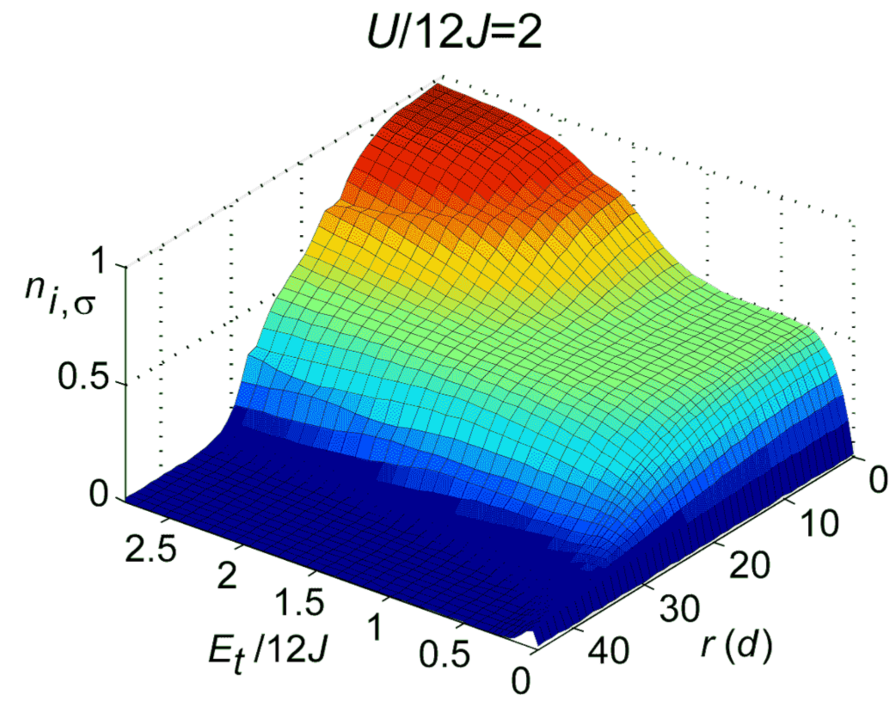

$T = 0.15t$

Additional plateau/kinks at $n_\sigma \approx 0.8$ for $T = 0.15t$ [Rosch group, courtesy of U. Schneider]

However: experimental temperatures are high $\rightsquigarrow$ advantage for QMC!

Real-space DMFT results for paramagnetic phase: QMC vs. NRG

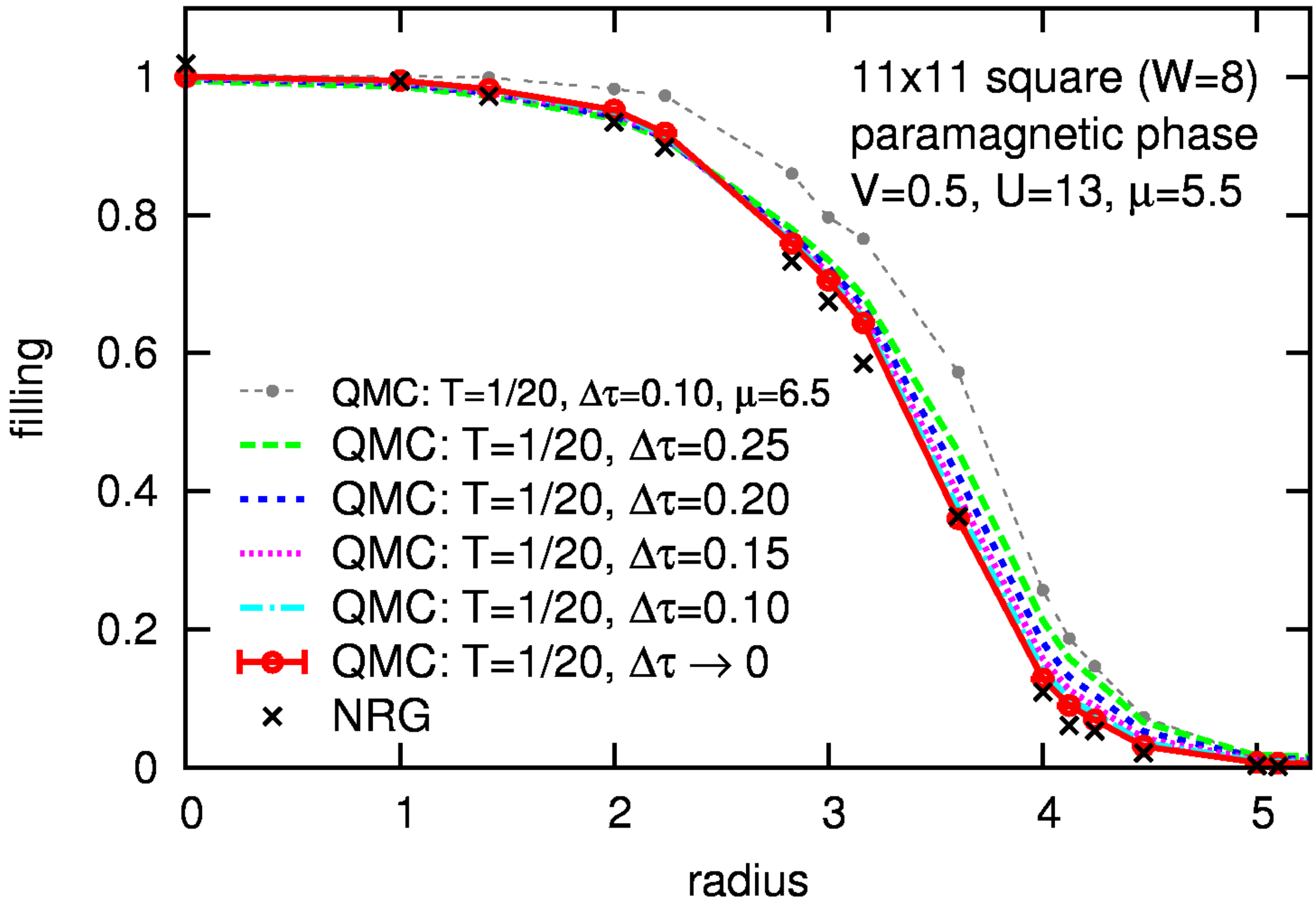

Good agreement QMC $\leftrightarrow$ NRG (after choosing same μ)

[NRG data by I. Titvinidze (collaboration within SFB/TR 49)]

Real-space DMFT results for AF phase: QMC vs. NRG

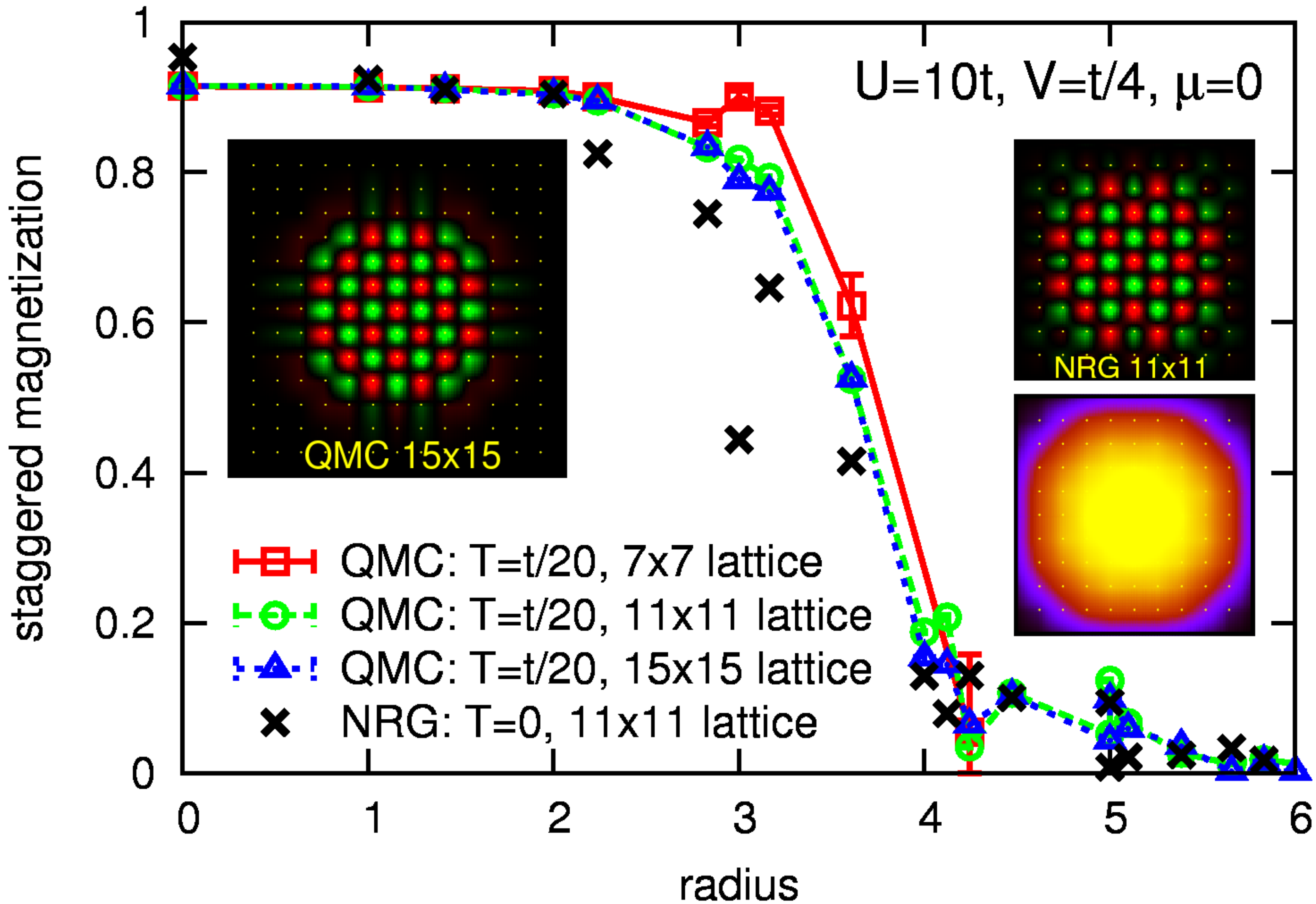

Finite-size effects surprisingly small; QMC apparently more accurate (even at low T)

Melting of a central antiferromagnetic phase

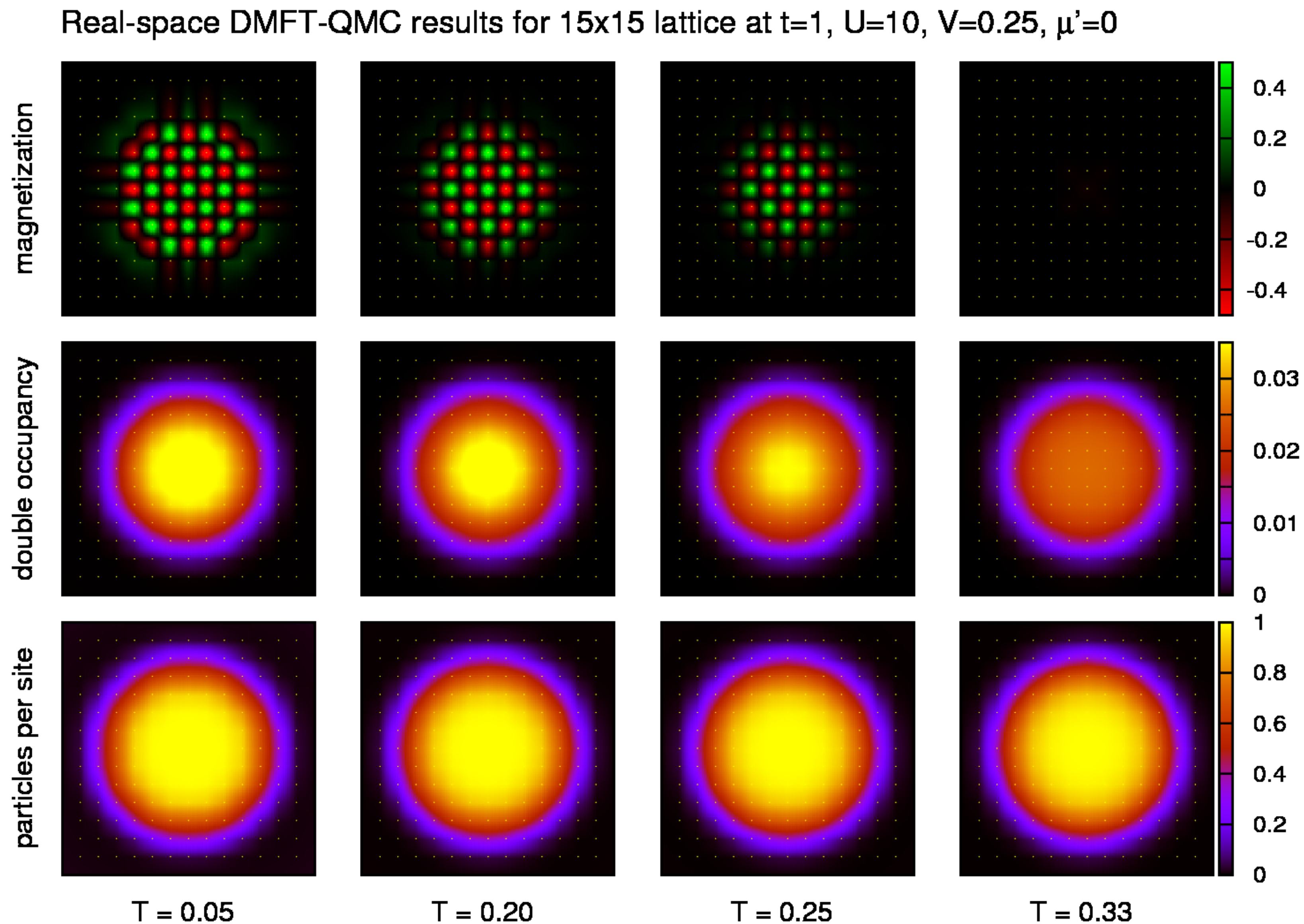

Antiferromagnetic order signaled by enhanced double occupancy

Effect of filling on the antiferromagnetic phase

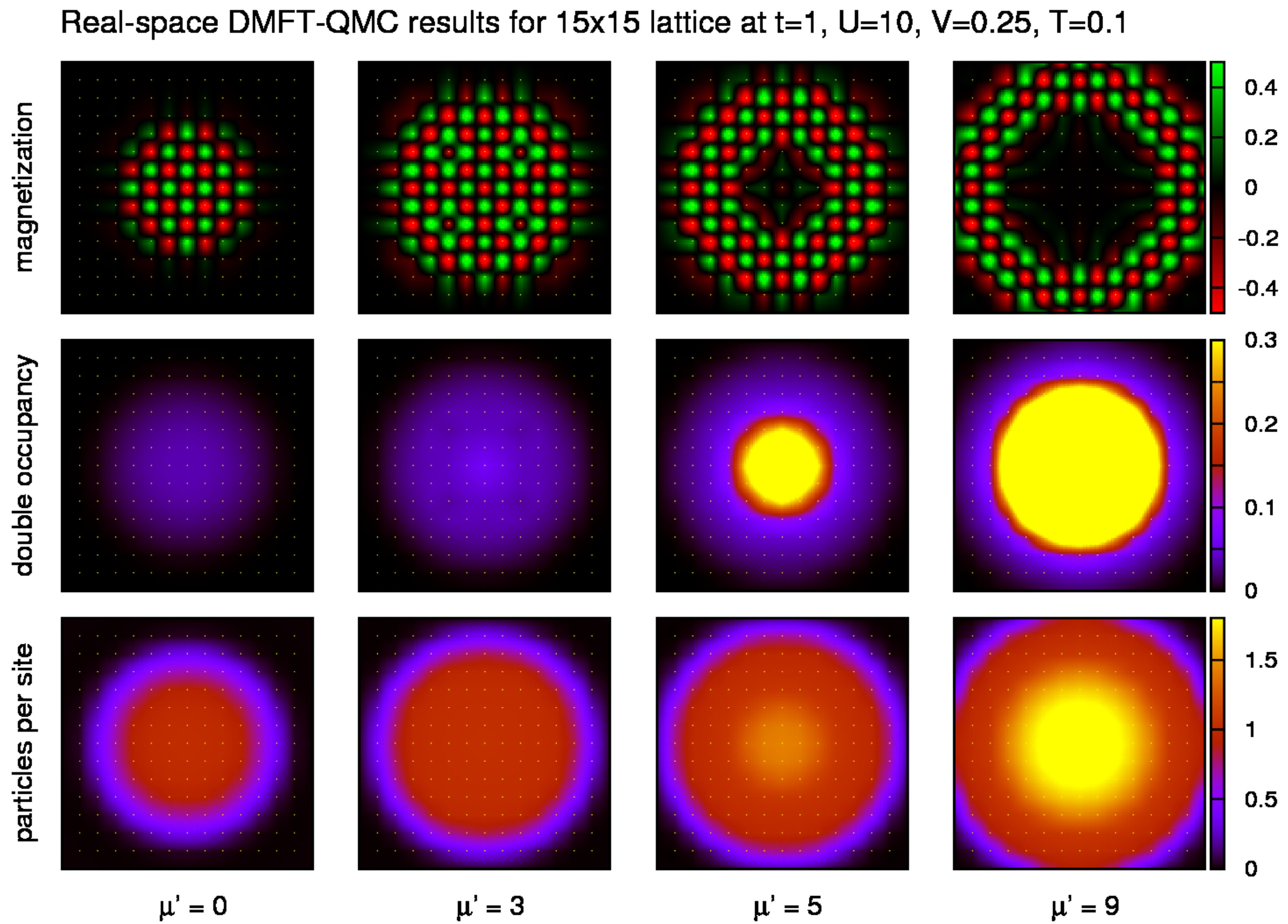

Buildup of metallic core → AF ring/shell

Effect of imbalance on the antiferromagnetic phase

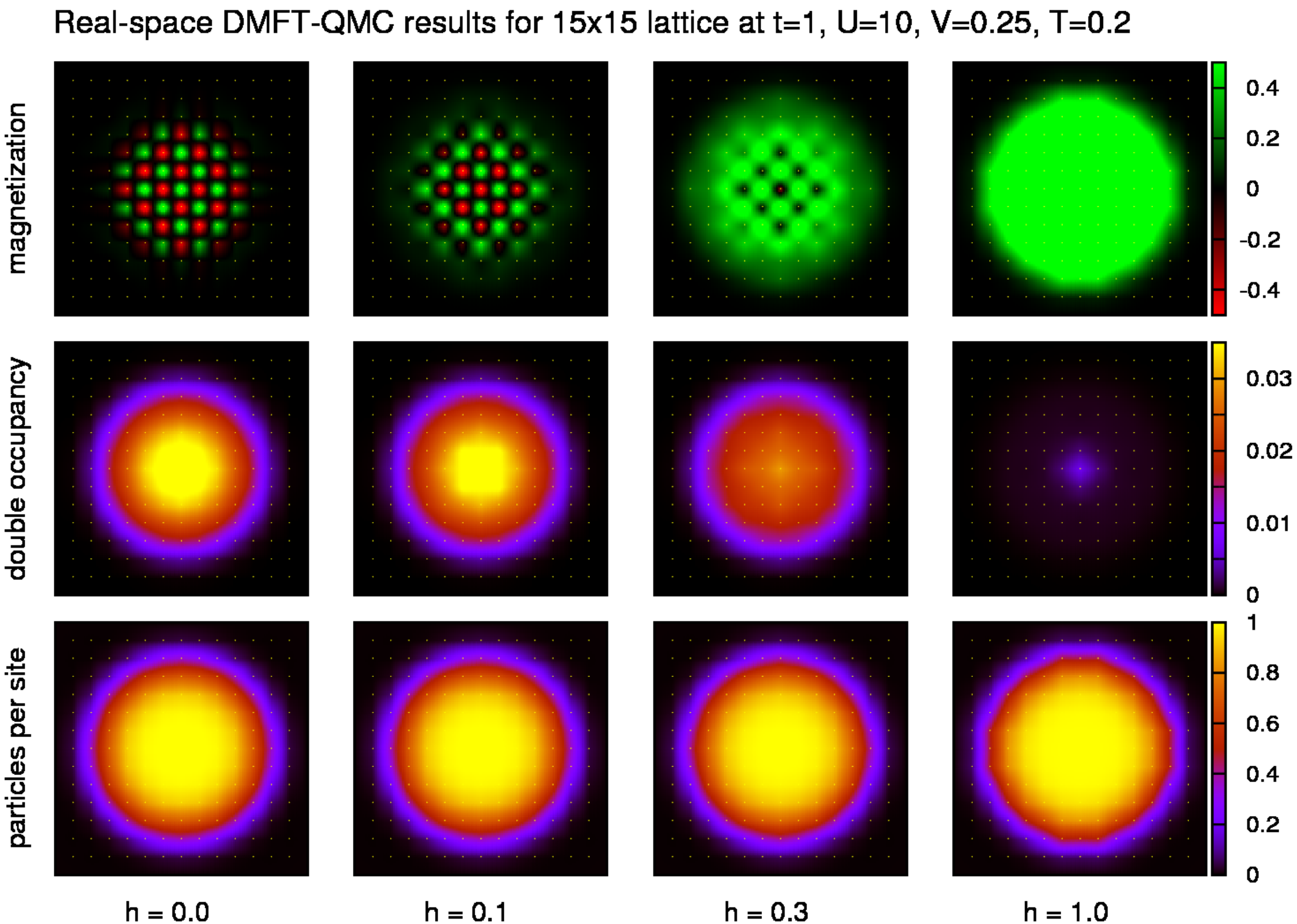

AF survives strong imbalance ($h = 0.3$); $h = 1$ nearly fully polarized

RDMFT-QMC

- arbitrary:
  - potential (also periodic, modulated,with impurities, missing sites etc.)
  - hopping matrix + lattice topology
  - dimension (within DMFT)
  - number of flavors and bands
  - precision (cheap with multigrid)
- wide temperature range
- ordered phases can be suppressed
- scales to thousands of sites/particles
- todo:
  - integrated multigrid $\Delta\tau$ extrapolation
  - energy $\longrightarrow$ entropy, free energy

Summary

Multigrid HF-QMC method: numerically exact (quasi CT) + efficient

Mott transition for 3 degenerate flavors in (U, T, μ) space

Novel semi-compressible phase

Bethe lattice approximation surprisingly accurate

Real-space DMFT

Efficient and flexible RDMFT-QMC code

Melting of an antiferromagnet, imbalance, LDA deficient

Outlook

3D calculations for realistic trap parameters and system sizes

Inequivalent spins/flavors: OSMT-like physics, ordered phases

Impact of higher Bloch bands

Spin-off: solids with large unit cells (distortions, surfaces, impurities, . . .)

Dependence of pair occupancy D on the lattice type

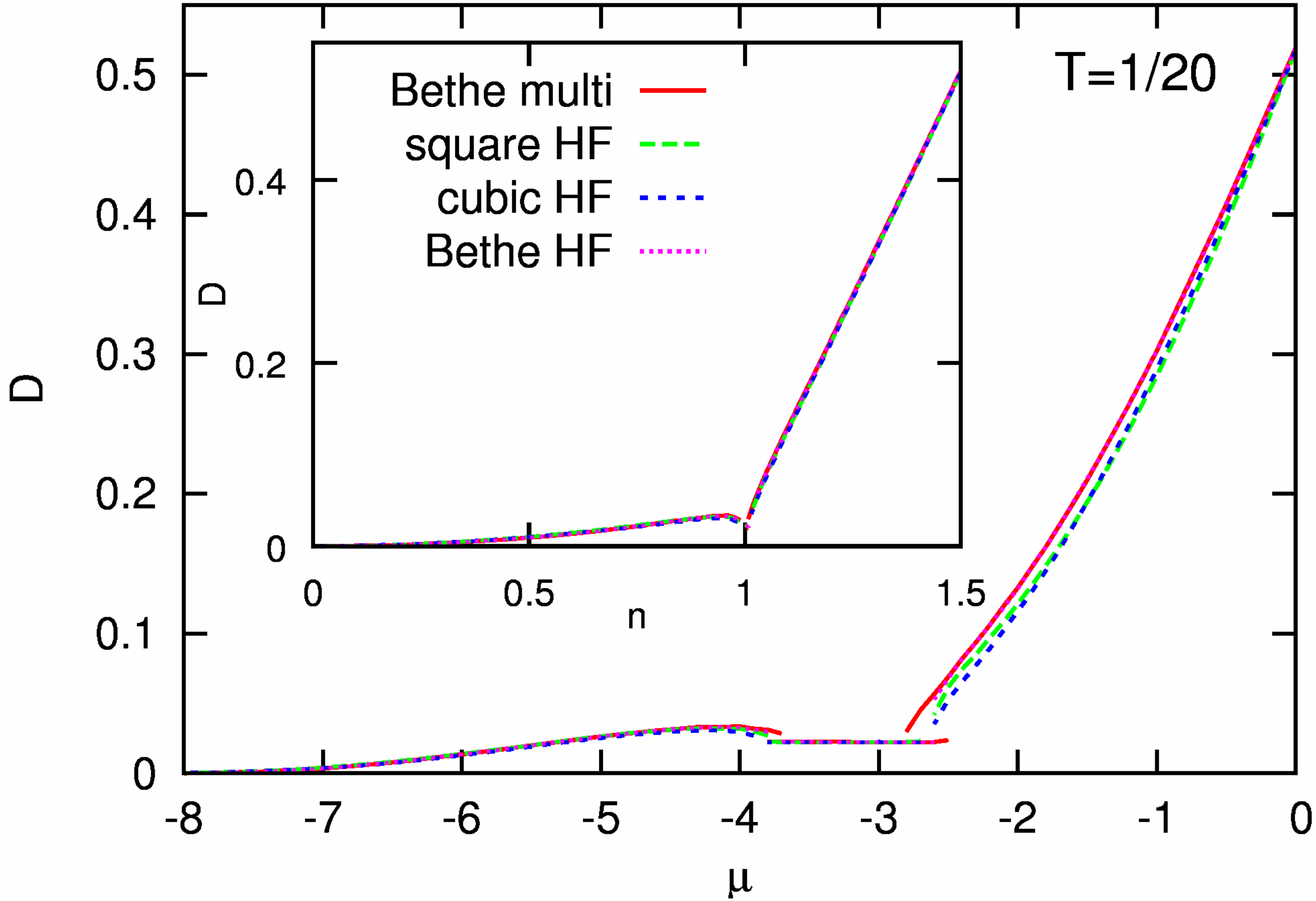

- Small differences in $D(\mu)$ curves are due to the density effects
- $D(n)$ curves are identical within the line width

RDMFT: strong proximity effects (not in local μ approximation)

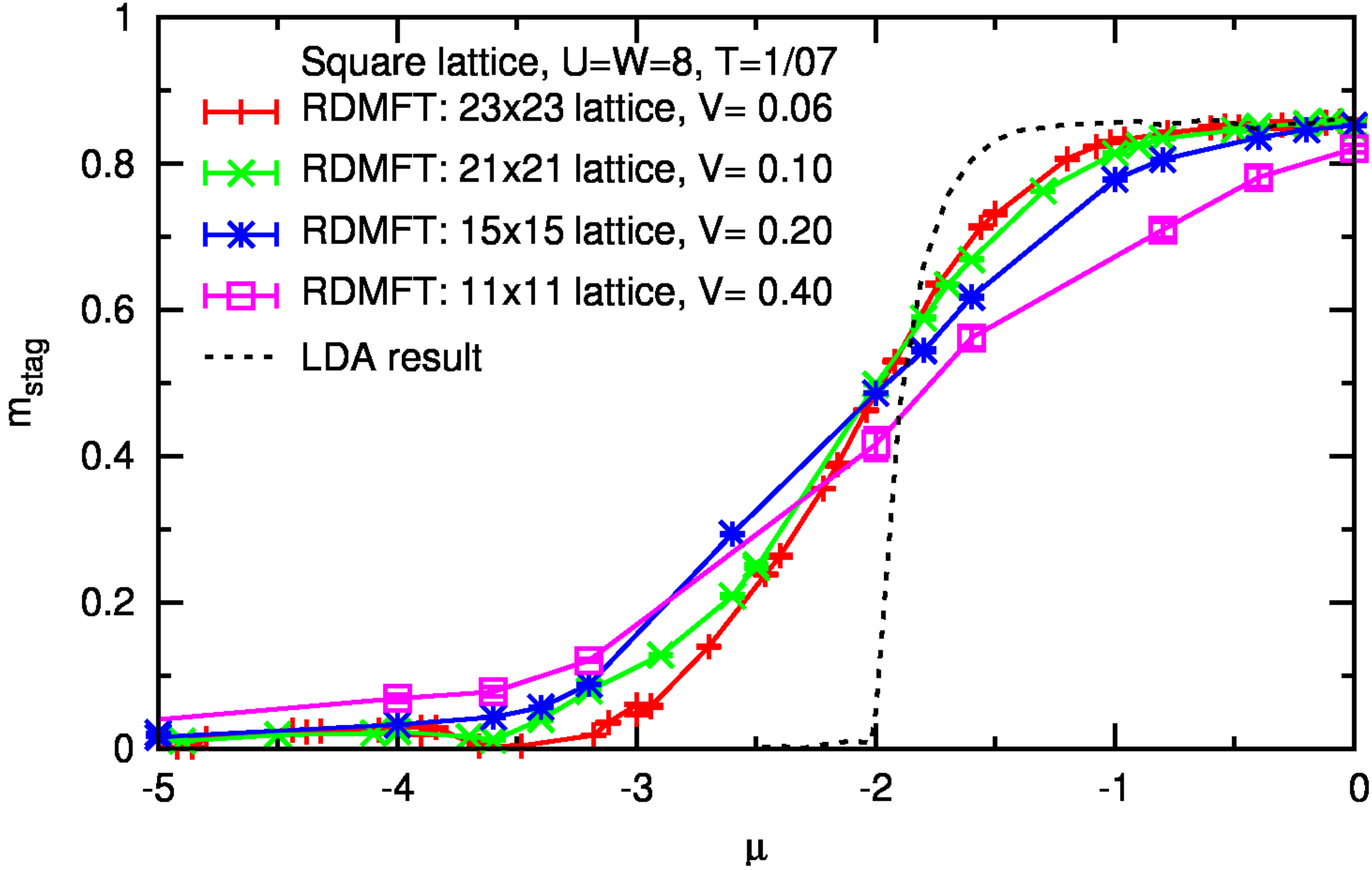

RDMFT: fast/slow convergence depending on initialization

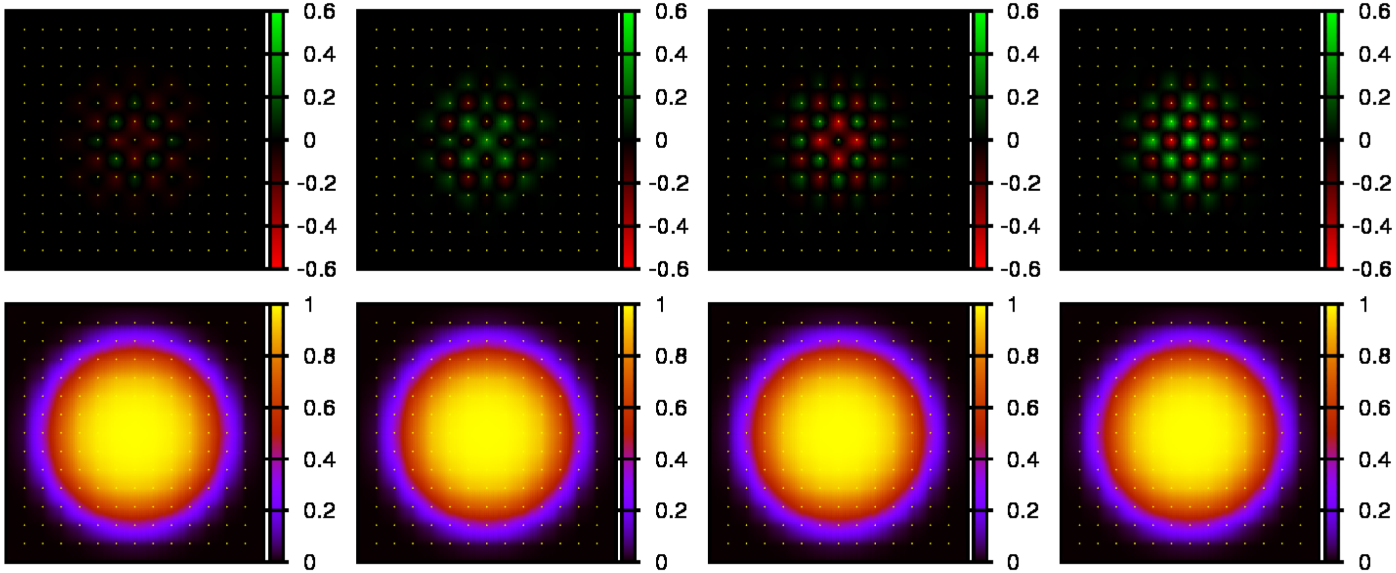

U=10, V=0.25, T=1/5, its 5-8

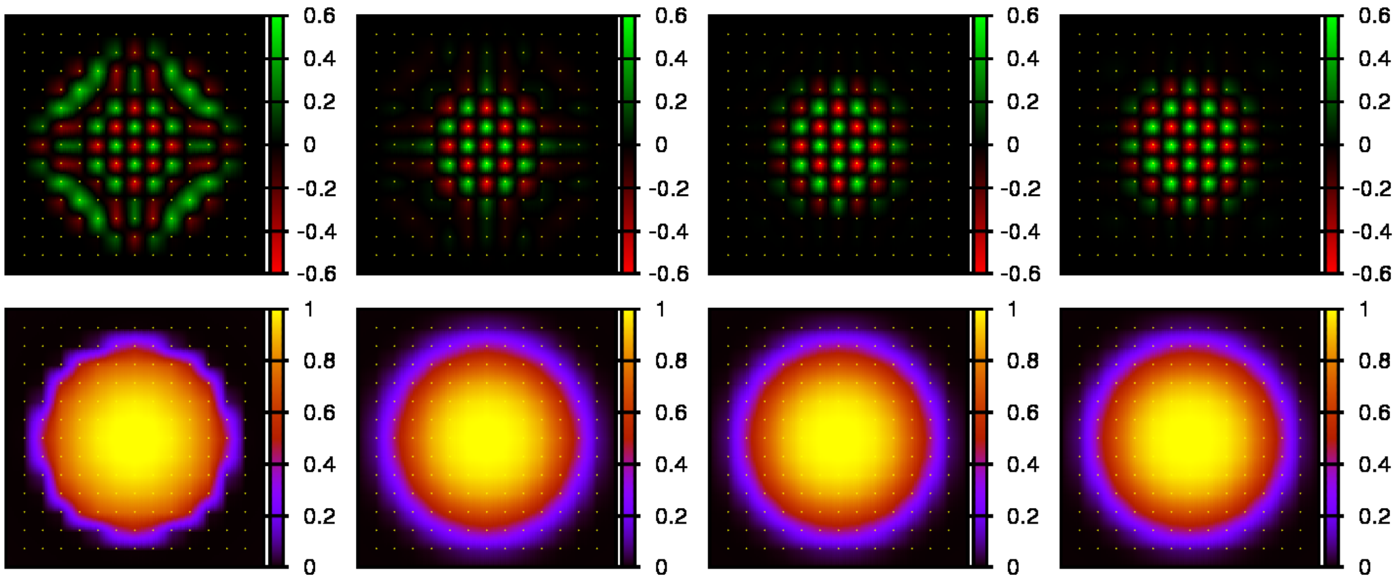

U=8, V=0.2, T=1/7, its 1-5

Efficiency: potential energy $E_{pot} = UD$ (at $U = W = 4$)

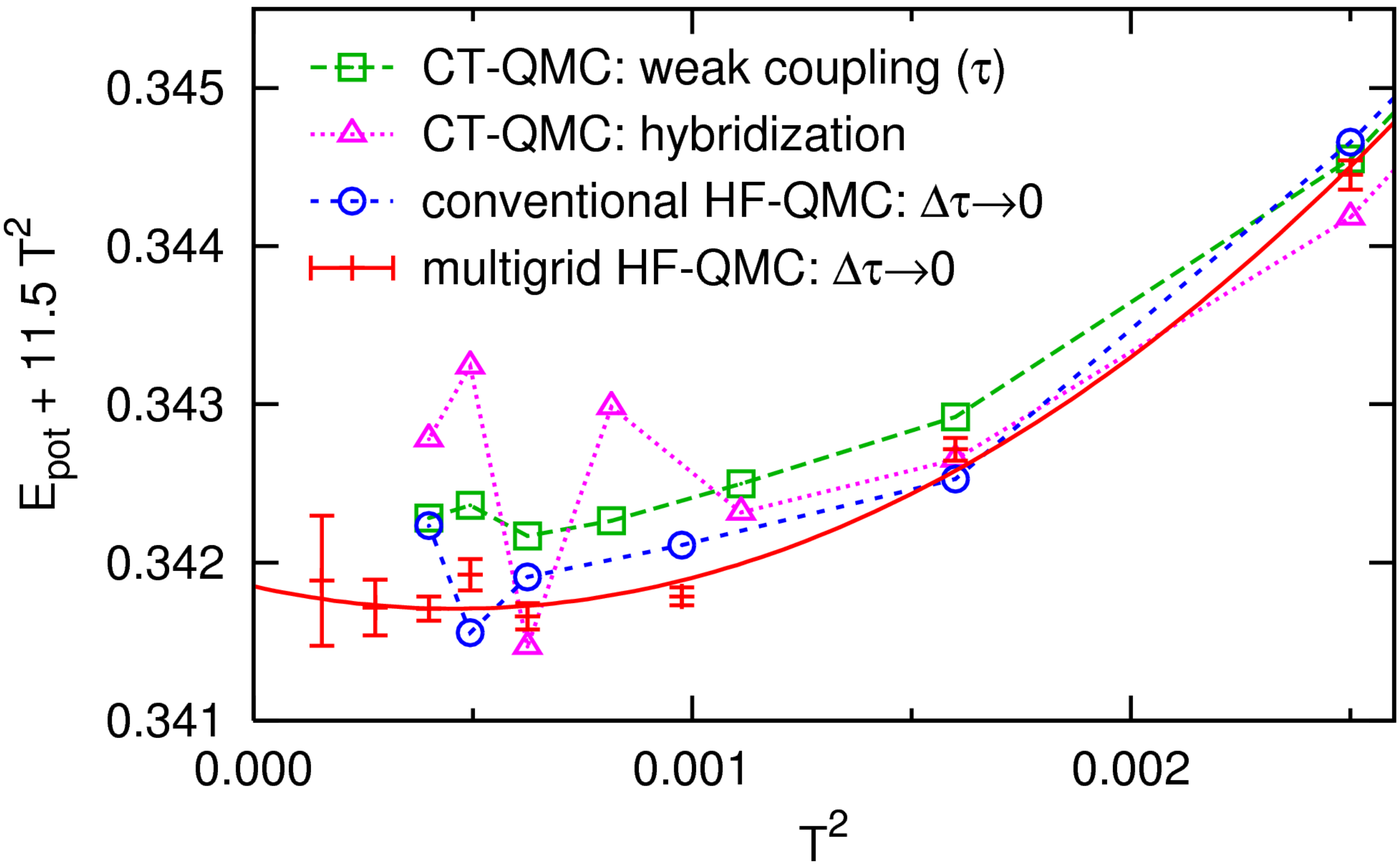

No more “difficult observables” for multigrid HF-QMC

Higher precision than CT-QMC methods at same effort

Result: unbiased, numerically exact Green function

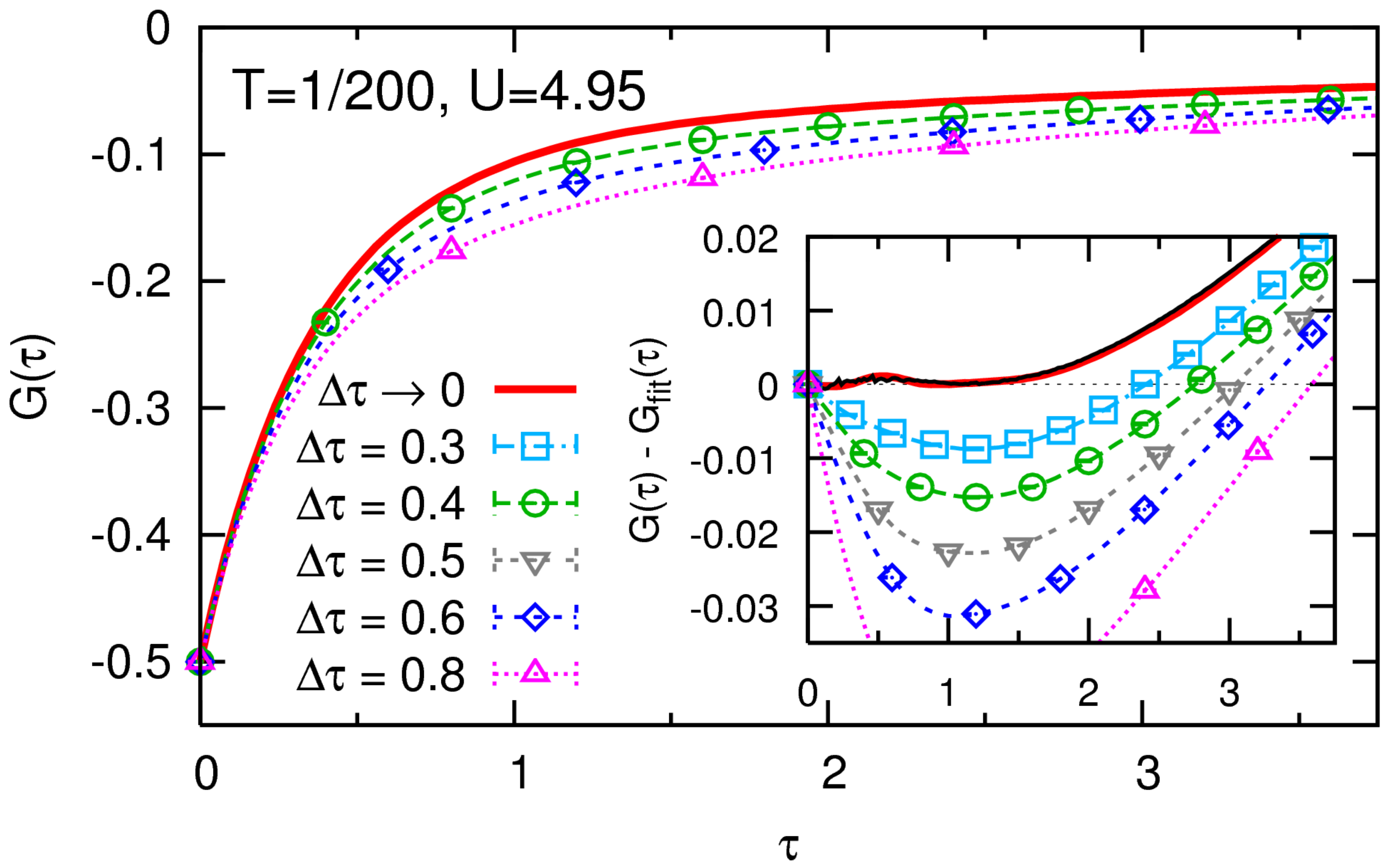

[NB, arXiv:0712.1290]

Excellent agreement with hybridization expansion CT-QMC [Werner et al., PRL (2006)]